Gulf of Mexico Gas Hydrate Joint Industry Project Leg II:
Green Canyon 955 LWD Operations and Results

Gilles Guerin[1], Ann Cook[1], Stefan Mrozewski[1], Timothy Collett[2], & Ray Boswell[3]

Introduction

Three holes, Green Canyon 955-I (GC 955-I), Green Canyon 955-H (GC 955-H), and Green Canyon 955-Q (GC 955-Q) were drilled in the Gulf of Mexico Green Canyon Block 955 to test the potential occurrence of gas hydrate in sand sediments associated with a channel/levee system at the mouth of the Green Canyon (Hutchinson *et al*., 2009). Hole GC 955-I was drilled in what was thought to be a thick part of a channel levee with a high potential for sand occurrence. Holes GC 955-H and GC 955-Q were drilled within a four-way closed structure which was thought to trap gas sourced along numerous local faults. A complete assessment of the Green Canyon 955 sites and a full description of the drilling operations are provided in McConnell *et al.* (2009) and Collett *et al.* (2009).

Operations

Logging-while-drilling (LWD) operations at the Green Canyon Block 955 Site were conducted using a state of the art bottom hole assembly (BHA), using the Schlumberger MP3, geoVISION, EcoScope, sonicVISION and PeriScope tools. For detailed description of the BHA, of each tool and of the tool measurements, see Mrozewski *et al*. (2009).

Hole GC 955-I

After tagging the seafloor at a driller's depth of 6822 ft below rig floor (fbrf), Hole GC 955-I was spudded at 11h15 on April 22, 2009. Following a spud protocol designed to maintain good conditions at the top of the hole (Collett *et al.*, 2009), the first 95 ft below seafloor (fbsf) were drilled while circulating 200 gallons of sea water per minute (gpm) and rotating the drill bit with only 15 rotations per minute (rpm). Between 95 and 160 fbsf, the drilling fluid flowrate was increased to 225 gpm and rotation rate to 75 rpm, after which they were increased to 350 gpm and 90 rpm, respectively. The rate of penetration (ROP) averaged ~250 ft/hr.

Drilling continued smoothly with drilling fluid sweeps every couple stands until 1275 fbsf when ROP was reduced to 180 ft/hr for the target zone of interest. At the same time, drilling fluid was swapped over to 10.5 pound per gallon (ppg) water-based drilling fluid to facilitate cuttings removal and borehole stability as the hole deepened. At 1310 fbsf, rotary speed increased to 140 rpm, and at 1875 fbsf, ROP was restored to 250 ft/hr for the remaining of the well. The total depth of 2203 fbsf was reached at 05h45 on April 23. The hole was not displaced with heavy drilling fluid since the deepest part of the hole had been drilled with a 10.5 gpm drilling fluid, but an LWD downlink was performed to slow the tools' record rates before the bottom hole assembly (BHA) was pulled out of hole and suspended in open water for the rig move to the next drill location.

Subsequent visual monitoring of the GC 955-I wellhead with the *Q-4000's* ROV revealed that the well was flowing water (no evidence of gas). To stop the observed water flow it was decided to place a cement plug in the well (for further discussion, see Collett *et al*., 2009). The LWD BHA was brought to surface by 23h30 and laid down shortly after. A simple BHA, without the LWD tools, was run back into the hole to place the cement plug.

Hole GC 955-H

After completing operations in Hole GC 955-I, the *Q-4000* was moved to the next drill location: Hole GC 955-H. Operations started at 2130 hr on April 24, with rigup and running the drill pipe and the LWD BHA to the seafloor. After tagging the seafloor at a driller's depth of 6721 fbrf, Hole GC 955-H was spudded at 06h30 on April 25, 2009. Following a spud protocol designed to maintain good

[1]Borehole Research Group
Lamont-Doherty Earth Observatory
of Columbia University
Palisades, NY 10964
E-mail:
Cook: acook@ldeo.columbia.edu
Guerin: guerin@ldeo.columbia.edu
Mrozewski: stefan@ldeo.columbia.edu

[2]US Geological Survey
Denver Federal Center, MS-939
Box 25046
Denver, CO 80225
E-mail:
tcollett@usgs.gov

[3]National Energy Technology Laboratory
U.S. Department of Energy
P.O. Box 880
Morgantown, WV 26507
E-mail:
ray.boswell@netl.doe.gov

borehole conditions at the top of the hole (Collett *et al.*, 2009), the first 10 fbsf were drilled while circulating 200 gpm of seawater and rotating the drillstring at 10 rpm. Between 10 and 180 fbsf, the pump flowrate was increased to 250 gpm and the rotation rate was increased to 55 rpm, after which point they were increased to 350 gpm and 90 rpm, respectively. At 650 fbsf, rotary speed was increased to 120 rpm. Above 1100 fbsf the ROP was targeted at 300 ft/hr.

Drilling continued smoothly with drilling fluid sweeps every few stands until 1100 fbsf when ROP was reduced to 180 ft/hr for the target zone of interest. At the same time, drilling fluid was changed to a 10.5 ppg water-based drilling fluid in anticipation of more difficult drilling. One hundred feet deeper, rotary speed was increased to 135 rpm in response to a developing problem with torque on the drill string. At 1520 fbsf, ROP and rotary speed were increased again to 300 ft/hr and 120 rpm, respectively. A total depth of 1936 fbsf was reached at 23h20 on April 25. The hole was displaced with 13.0 ppg drilling fluid before the BHA was pulled out of hole and suspended in open water in preparation for the rig move. The BHA cleared the seafloor at 03h00, April 26, after a camera survey had ensured that the hole was not flowing, and the rig was moved to the next location.

Hole GC 955-Q

After completing the short move to GC 995-Q location, operations started with the tagging the seafloor at a driller's depth of 6567 fbrf, and spudding Hole GC 955-Q at 14h15 on April 26, 2009. Following a spud protocol designed to maintain good conditions, the first 65 fbsf were drilled while circulating seawater at a low flow rate of 200 gpm and bit rotate rate of only 15 rpm. Between 65 and 170 fbsf, pump flowrate was increased to 250 gpm and bit-rotation was increased to 50 rpm, after which point they were increased to 350 gpm and 105 rpm, respectively. For the first 190 fbsf the rate of penetration was highly variable and averaging roughly 600 ft/hr, but it was later stabilized to the target ROP of 400 ft/hr.

Drilling continued smoothly with drilling fluid sweeps every couple of stands until 930 fbsf when rotary speed was increased to 135 rpm in response to drilling conditions. At 1238 fbsf, the ROP was reduced to 180 ft/hr for the target zone of interest. At the same time, drilling fluid was changed from seawater to a 10.5 pound per gallon (ppg) water-based drilling fluid.

When making a connection at 1516 fbsf at 00h04 on April 27, shortly after real-time LWD measurements had indicated the bit had reached a hydrate-bearing formation, the *Q-4000* ROV observed a gas release from the wellhead. Drilling protocols established prior to the expedition required that the flow be controlled and the well abandoned and cemented. The well was initially filled with a 13.0 ppg drilling fluid. After observing no flow from the well for over an hour, the LWD BHA was slowly pulled out of hole in anticipation of running a cementing BHA to plug and abandon the well. The ROV observed a new gas bubble stream from the well. After running in hole and tagging an apparent bridge at 743 fbsf, the well was displaced with two borehole volumes of 16.0 ppg drilling fluid. The well continued to flow intermittently and after two more displacements of 16.0 ppg drilling fluid, the LWD BHA was pulled to surface and laid down by 18h45 on April 27 before running in with the cementing BHA. Further details on the operations in the Green Canyon 955 Block are provided in Collett *et al*. (2009).

Data Quality

Hole GC 955-I

Figure F1 displays selected parameters that illustrate the drilling process in Hole GC 955-I and its possible influence on data quality.

The increase in residual pressure (annulus pressure after subtraction of hydrostatic pressure) and equivalent circulating density (ECD, a similar measure) at ~1275 fbsf is the result of an increase in the drilling fluid density that was necessary to support the drilling (see ***Operations*** above). No changes in pressure were observed that would have suggested the release of free gas or any other hazard.

Averaged over 5 ft depth intervals, the ROP log has cyclical spikes that are artifacts due to speed, depth, and/or depth tracking fluctuations occurring immediately before, during and after pipe connections (Figure F1). The ROP spikes occasionally correspond with smeared horizontal lines on the geoVISION resistivity images that are observed 60 ft higher up the hole due to the depth difference between where the measurements are made in hole. Dark, incongruous pixelation occurs on the resistivity images in high-resistivity zones. These pixels are null values in the raw data, a result of a problem in the current geoVISION software.

The EcoScope geochemical logs were the only logs affected by the high ROP. The geochemical logs were not properly calibrated, and thus none of the geochemical logs report reliable measurements. Ultrasonic and density calipers reveal only moderate near-seafloor borehole enlargement. Below 270 fbsf, the hole is in very good shape and rarely exceeds 8.75 inches in diameter. Notable washouts, where density and porosity data are unreliable, occur in the sandy intervals below 1190 fbsf.

EcoScope data are only acquired once flow past the MWD turbine is sufficient to power the tool, which in GC 955-I occurred at 80 fbsf for density measurements (Figures F2 and F3). When the minitron is on, the geoVISION's gamma ray reads appreciably higher than the EcoScope's because it is not compensated for minitron-induced oxygen activation.

The depths relative to seafloor were fixed by identifying the step change in the geoVISION gamma ray log at the seafloor. For Hole GC 955-I, the gamma ray log identified the seafloor at 6823 fbrf, 1 ft below the initial depth estimated by the drillers. The rig floor logging datum was located 52 ft above sea level.

Hole GC 955-H

Figure F4 displays selected parameters that illustrate the drilling process for Hole GC 955-H and its possible influence on data quality.

The only changes observed in borehole pressure were due to the increase in drilling fluid density at 1080 fbsf, and to the several drilling fluid sweeps that were made to support drilling.

The log for rate of penetration, averaged over 5 ft depth intervals, indicates cyclical spikes that are artifacts due to speed, depth, and/or depth tracking fluctuations occurring immediately before, during and after pipe connections. The ROP spikes occasionally correspond with smeared horizontal lines on the geoVISION resistivity images that are offset by 60 ft higher up the hole. The images are also marred by dark, incongruous pixilation in high-resistivity zones; these are manifestations of null values in the raw data, that result from errors in the current geoVISION software.

Ultrasonic and density calipers, as well as the resistivity images, reveal typical near-seafloor borehole enlargement. Below 275 fbsf, the hole is in very good condition and rarely exceeds 8.75 inches in diameter. A notable washout, where density and porosity data are unreliable, occurs in the sandy interval between 1280 to 1600 fbsf.

EcoScope data are only acquired once flow past the MWD turbine is sufficient to power the tool, which in GC 955-H occurred at 100 fbsf for density measurements (Figures F5 and F6). When the minitron is on, the geoVISION's gamma ray reads appreciably higher than the EcoScope's because it is not compensated for minitron-induced oxygen activation.

The geoVISION gamma ray log identified the seafloor in Hole GC 955-H at 6718 fbrf, 3 ft above the initial depth estimated by the drillers. The rig floor logging datum was located 51 ft above sea level.

Hole GC 955-Q

Figure F7 displays selected parameters that illustrate the drilling process for Hole GC 955-Q and its potential influence on data quality.

The only changes observed in borehole pressure curves were due to the several drilling fluid sweeps that were made to clean the hole, and to the increase in drilling fluid density at 1240 fbsf.

The ROP log is averaged over 5 ft depth intervals; the cyclical spikes are artifacts due to speed, depth, and/or depth tracking fluctuations occurring immediately before, during and after pipe connections. The ROP spikes occasionally correspond with subtle horizontal lines in the geoVISION resistivity image which appear 61 ft higher up the hole. The images are also marred by dark, incongruous pixilation in high-resistivity zones; these are manifestations of null values in the raw data, a result of a problem in the current geoVISION software. Depth tracking errors are also the likely cause of apparent EcoScope neutron data dropouts at 400, 600, 730 and 1044 fbsf, and of the EcoScope gamma ray spike at 518 fbsf.

The EcoScope geochemical logs were the only logs affected by the high ROP. The geochemical logs were not properly calibrated, and thus none of the geochemical logs report reliable measurements.

Ultrasonic and density calipers, as well as the resistivity images, reveal very moderate near-seafloor borehole

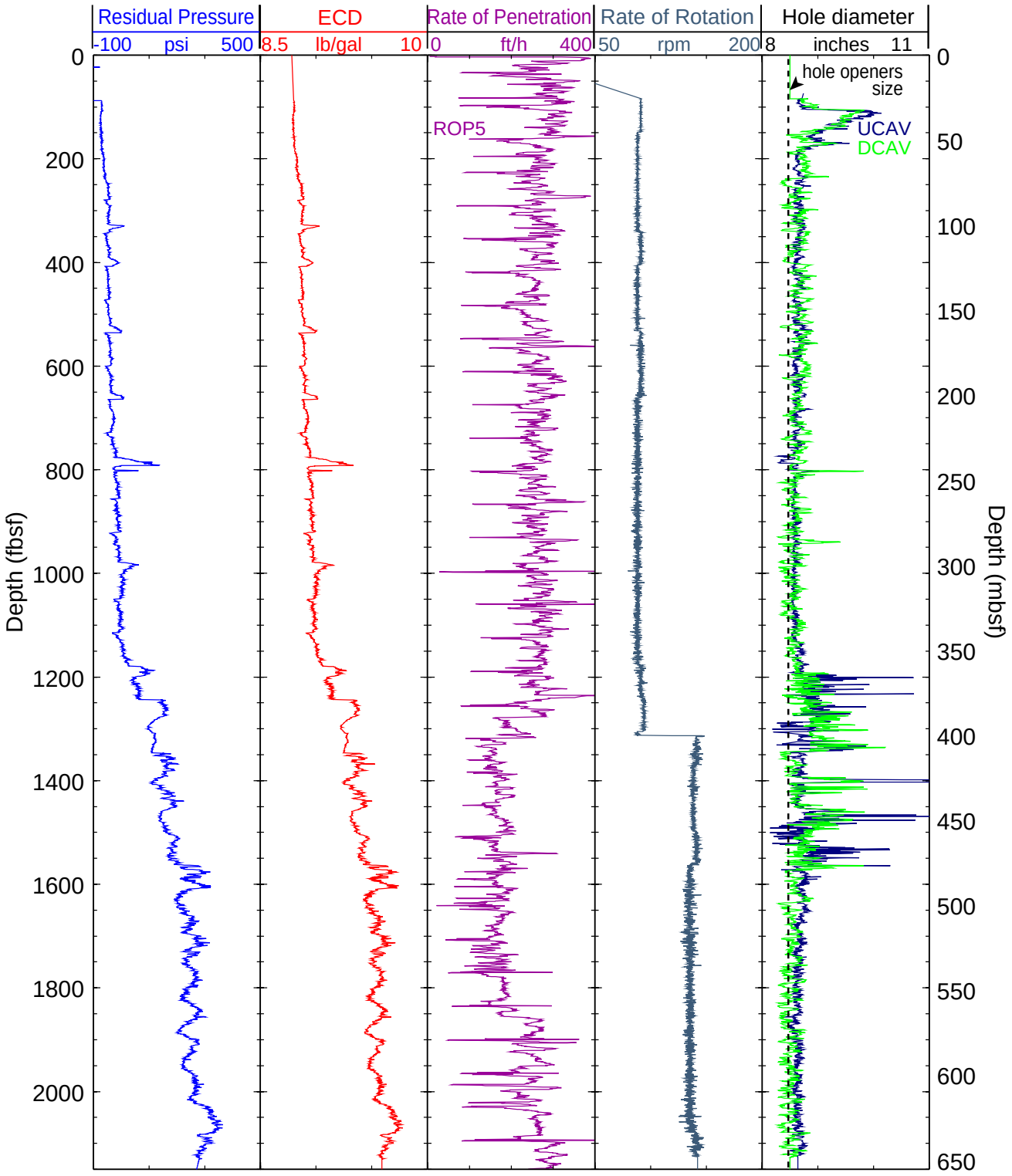

Figure F1: *Monitoring and quality control LWD/MWD logs from Hole GC 955-I. Residual Pressure = Pressure in the annulus after subtraction of the hydrostatic pressure; ECD = Equivalent Circulating Density = effective density of the fluid exerting pressure against the borehole formation; UCAV = Ultrasonic caliper, DCAV = Density caliper.*

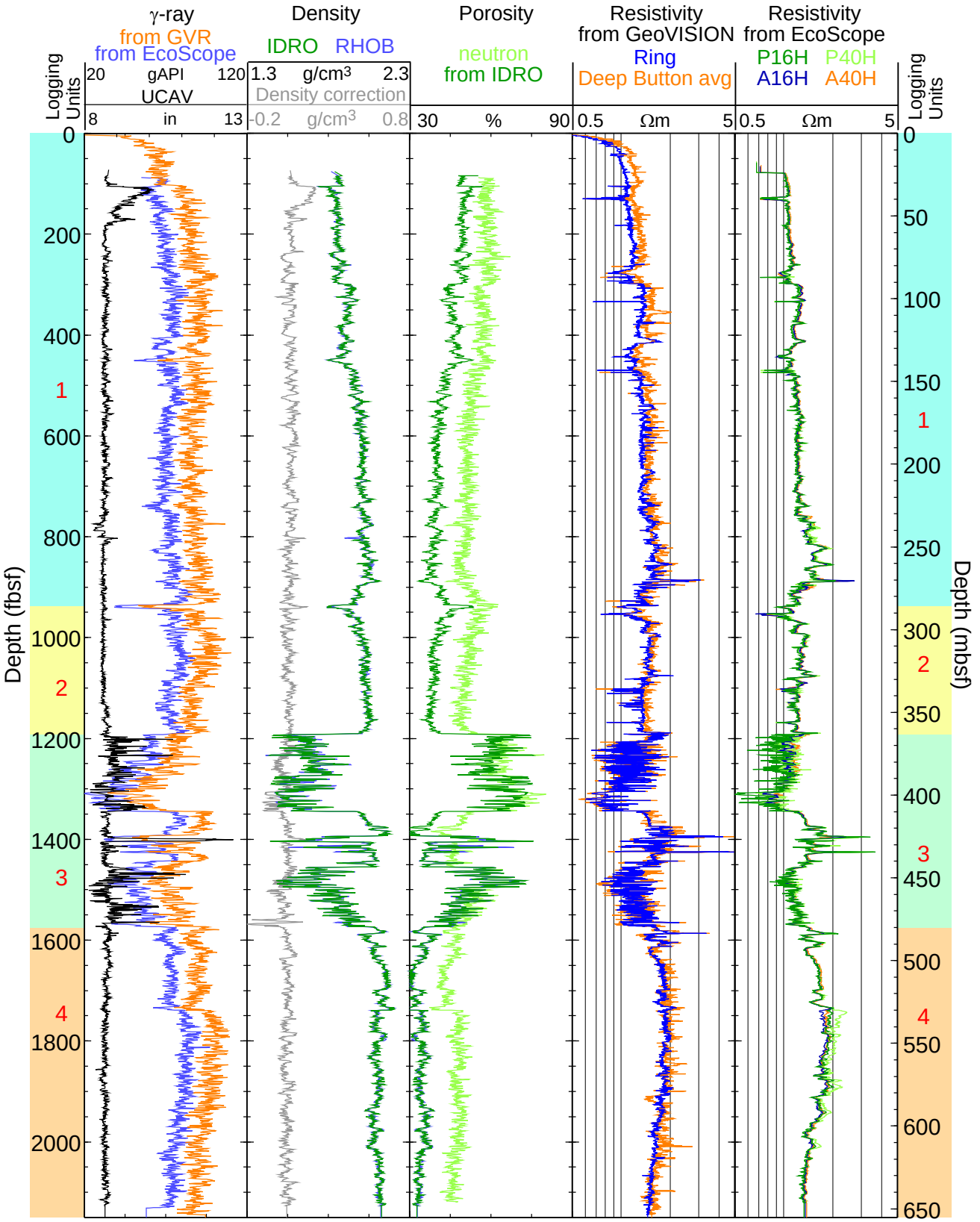

Figure F2: *Summary of LWD log data from Hole GC 955-I. gAPI = American Petroleum Institute gamma ray units, RHOB = Bulk density (EcoScope), IDRO = Image-derived density (EcoScope); neutron = "Best neutron porosity" (EcoScope); Ring = Ring resistivity (geoVISION); PXXH = Phase-shift resistivity at 2 MHZ and a transmitter-receiver spacing of XX inches (EcoScope); AXXH = Attenuation resistivity measured at 2 MHz and a transmitter-receiver spacing of XX inches (EcoScope). Logging units as described in this report are shown.*

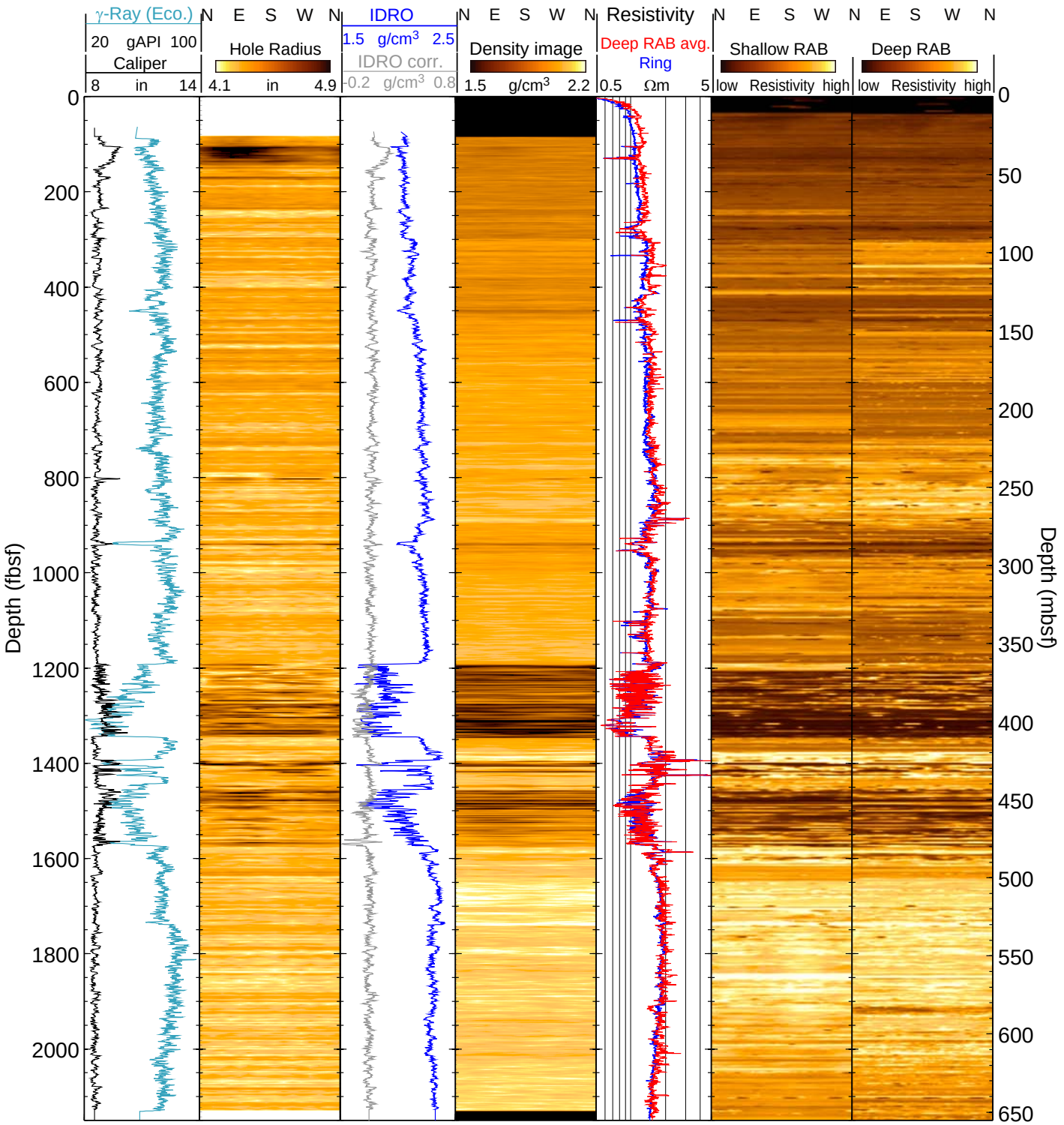

Figure F3: *LWD image data from Hole GC 955-I. gAPI = American Petroleum Institute gamma ray units; RAB = electrical image obtained by the geoVISION tool; IDRO = Image-derived density (EcoScope). The cardinal directions indicate orientation of the images.*

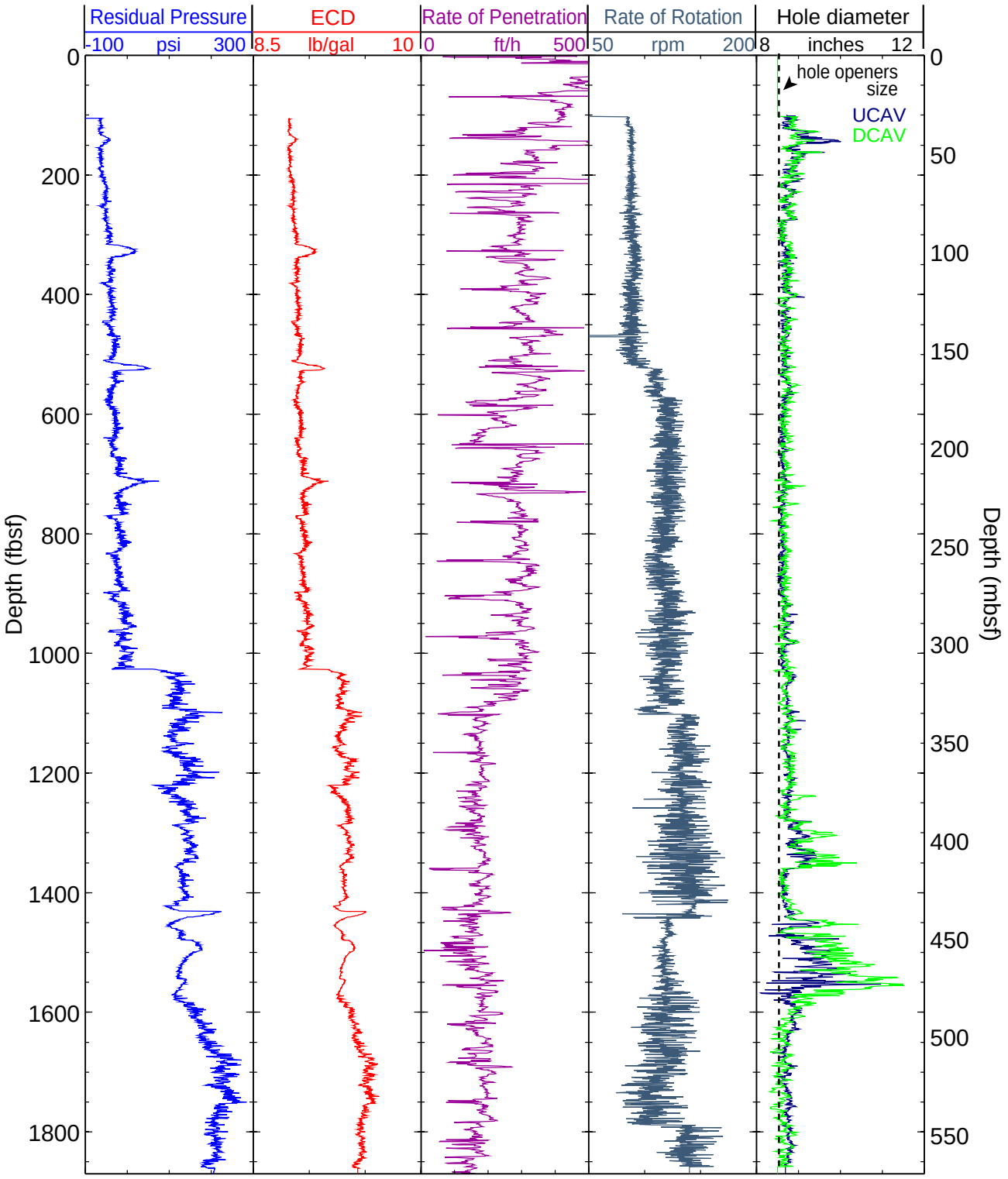

Figure F4: *Monitoring and quality control LWD/MWD logs from Hole GC 955-H. Residual Pressure = Pressure in the annulus after subtraction of the hydrostatic pressure; ECD = Equivalent Circulating Density = effective density of the fluid exerting pressure against the borehole formation; UCAV = Ultrasonic caliper, DCAV = Density caliper.*

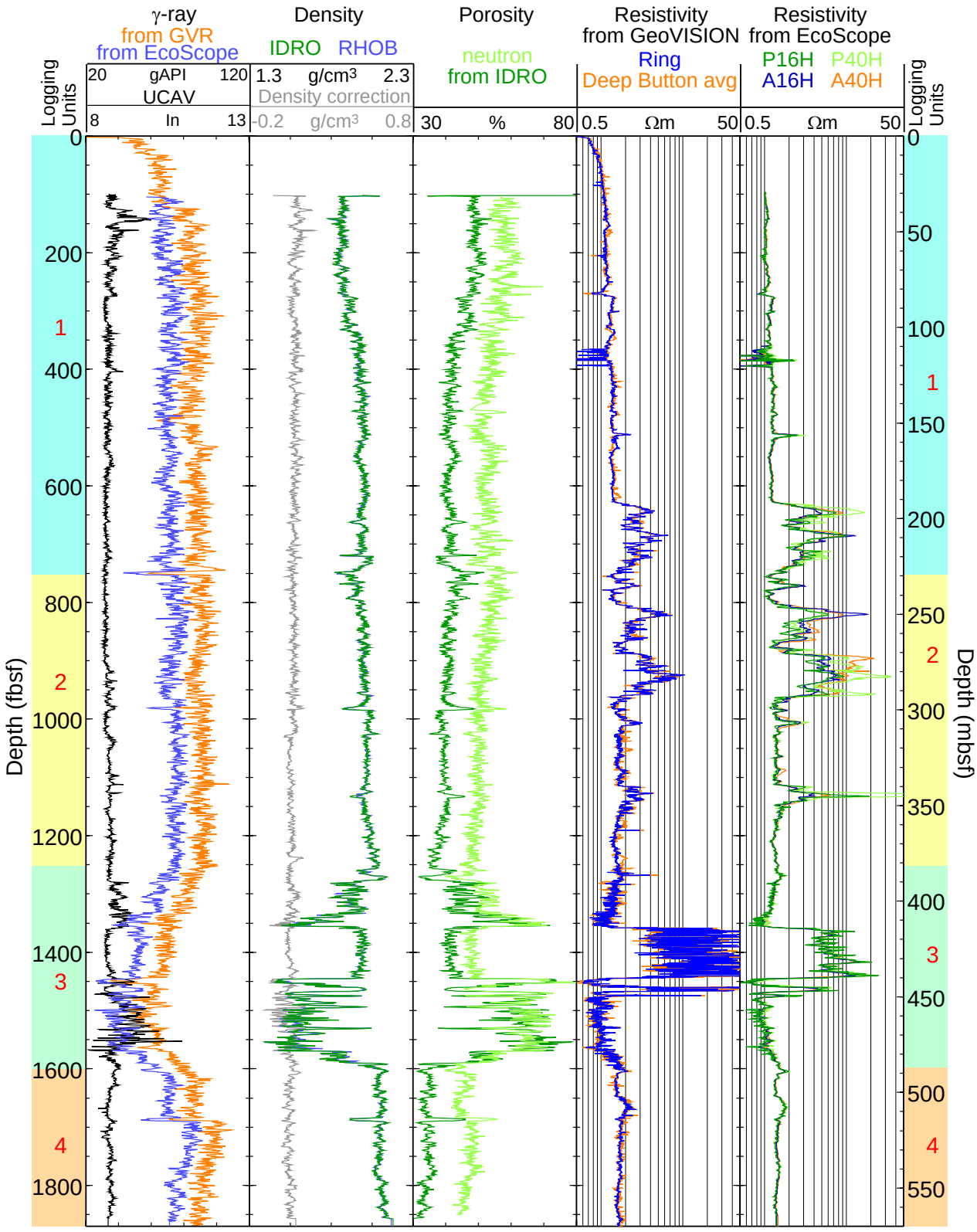

Figure F5: *Summary of LWD log data from Hole GC 955-H. gAPI = American Petroleum Institute gamma ray units, RHOB = Bulk density (EcoScope), IDRO = Image-derived density (EcoScope); neutron = "Best neutron porosity" (EcoScope); Ring = Ring resistivity (geoVISION); PXXH = Phase-shift resistivity at 2 MHZ and a transmitter-receiver spacing of XX inches (EcoScope); AXXH = Attenuation resistivity measured at 2 MHz and a transmitter-receiver spacing of XX inches (EcoScope). Logging units as described in this report are shown.*

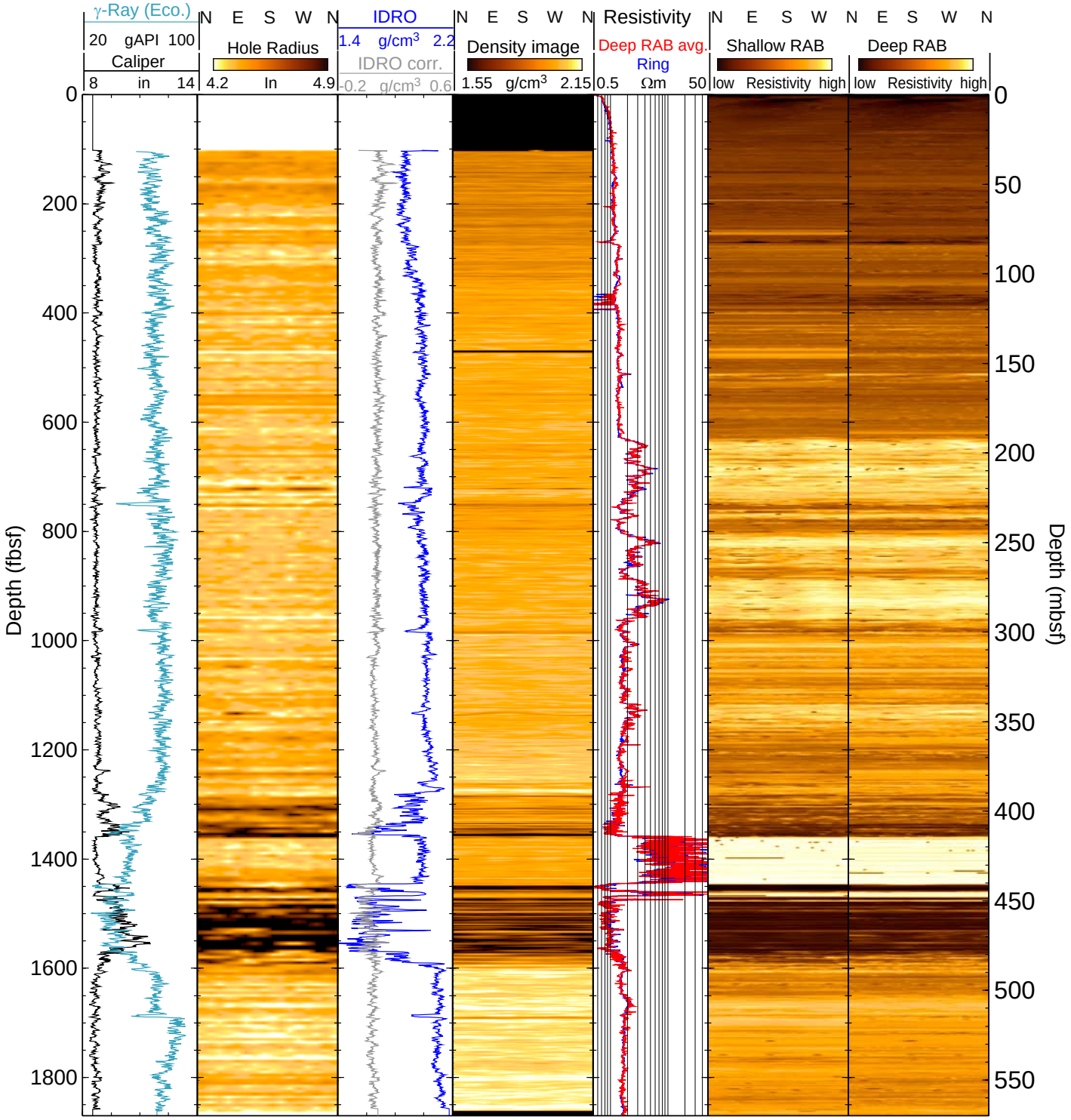

Figure F6: *LWD image data from Hole GC 955-H. gAPI = American Petroleum Institute gamma ray units; RAB = Electrical image obtained by the geoVISION tool; IDRO = Image-derived density (EcoScope). The cardinal directions indicate orientation of the images.*

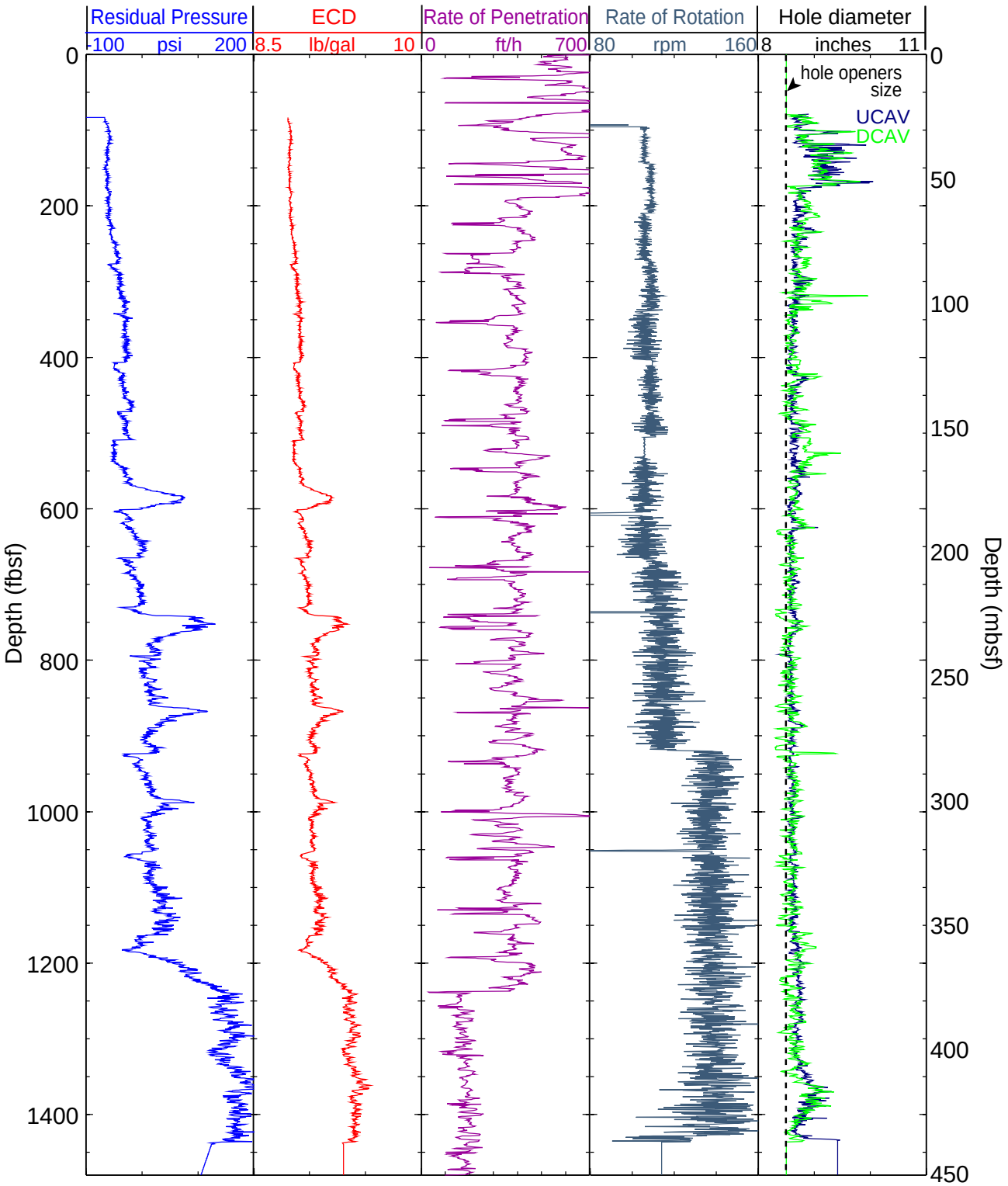

Figure F7: *Monitoring and quality control LWD/MWD logs from Hole GC 955-Q. Residual Pressure = Pressure in the annulus after subtraction of the hydrostatic pressure; ECD = Equivalent Circulating Density = effective density of the fluid exerting pressure against the borehole formation; UCAV = Ultrasonic caliper, DCAV = Density caliper.*

enlargement. Below 180 fbsf, the hole is in very good shape and rarely exceeds 8.75 inches in diameter. Notable washouts, where density and porosity data may be unreliable, occur at 320 fbsf and in the sandy interval below 1350 fbsf.

EcoScope data are only acquired once flow past the MWD turbine is sufficient to power the tool, which in Hole GC 955-Q occurred at 80 fbsf for density measurements (Figures F8 and F9). When the minitron is on, the geoVISION's gamma ray reads appreciably higher than the EcoScope's because it is not compensated for minitron-induced oxygen activation.

The geoVISION gamma ray log identified the seafloor in Hole GC 955-Q at 6565 fbrf, 2 ft above the initial depth estimated by the drillers. The rig floor logging datum was located 51 ft above sea level.

Interpretation of LWD Logs

Logging Displays Overview

The combined analysis of the different logs and images recorded by the LWD tools in Holes GC 955-I, GC 955-H, and GC 955-Q delineates several logging units with distinct trends or features that can be observed in the three wells drilled in Green Canyon Block 955. Some of these trends can be correlated to the seismic stratigraphy described in the GC 955 Site Summary (McConnell *et al.,* 2009).

Figures F2, F5, and F8 show the primary logs recorded by the geoVISION and the EcoScope tools in Holes GC 955-I, GC 955-H and GC 955-Q, respectively. As noted in the ***Data Quality*** section of this report, the offset between the gamma ray logs recorded by the two tools is the result of the influence of the gamma rays activated in the formation by the EcoScope minitron source on the geoVISION gamma ray measurements. Despite this offset, the two tools display identical trends, and only the EcoScope gamma ray will be used in the following discussion.

Figures F3, F6, and F9 give a summary of some of the images recorded by the geoVISION and the EcoScope tools. While showing the same measurements as the log curves, and allowing the same type of correlations, the azimuthal images illustrate the influence of structure and heterogeneity on the isotropic measurements captured by the logs. These images, and their implications for the nature of the distribution of gas hydrate, are described in greater retails in ***LWD Borehole Images*** and ***Gas Hydrate*** below.

Figures F10, F11, and F12 display the prelimiminary compressional velocity data recorded by the MP3 and the sonicVISION tools in Holes GC 955-I, GC 955-H and GC 955-Q, respectively. In addition to the V_p logs, the display of the monopole waveforms and of the slowness-time coherence (STC) projections used to derive V_p, provides an assessment of the quality of the acoustic data and of the attenuating effect of gas hydrate. The velocity profiles were refined by post cruise processing. Additional processing will be required to fully resolve differences between the velocity profiles produced by the two acoustic tools and ambiguous features such as the apparent low velocity at the bottom of Hole GC 955-Q which is likely due to poor waveform quality.

In all these figures, the gamma ray and resistivity curves provide a common indication to the variations in lithology and/or gas hydrate occurrence.

Logging Units

Logging Unit 1 extends from the surface to ~940 fbsf in Hole GC 955-I, to ~750 fbsf in GC 955-H, and to ~920 fbsf in Hole GC 955-Q. In the three holes, Unit 1 is characterized by a steady downward increase in density, resistivity and sonic velocity as well as a mostly uniform or slightly increasing gamma ray. Within this unit, in the three holes, a subtle step-like increase in velocity and resistivity between ~300 and 350 fbsf, depending on the hole, is likely related to Seismic Horizon A, marking the transition from marine clays to interbedded clays with sands below. The bottom of the unit is defined by a drop in velocity, resistivity and density that can be associated with seismic Horizon B (McConnell *et al.,* 2009) and by a thin (a few feet thick) clean sand layer encountered by the three holes at the base of the unit (~940 fbsf in Hole GC 955-I, ~750 fbsf in GC 955-H, and ~920 fbsf in GC 955-Q).

Characterized by mostly uniform resistivity (except for GC 955-H, which contains gas hydrate-filled fractures) and gamma ray baselines, with density and velocity increasing with compaction, Logging Unit 2 extends to ~1200 fbsf in GC 955-I, to ~1250 fbsf in GC 955-H, and to ~1350 fbsf in GC 955-Q. It corresponds mostly to sand dominated channel deposits between Horizons B and C. Resistivity is mostly uniform in this unit in Holes GC 955-I and -Q, but highly variable resistivity values between ~620 and 1000 fbsf in

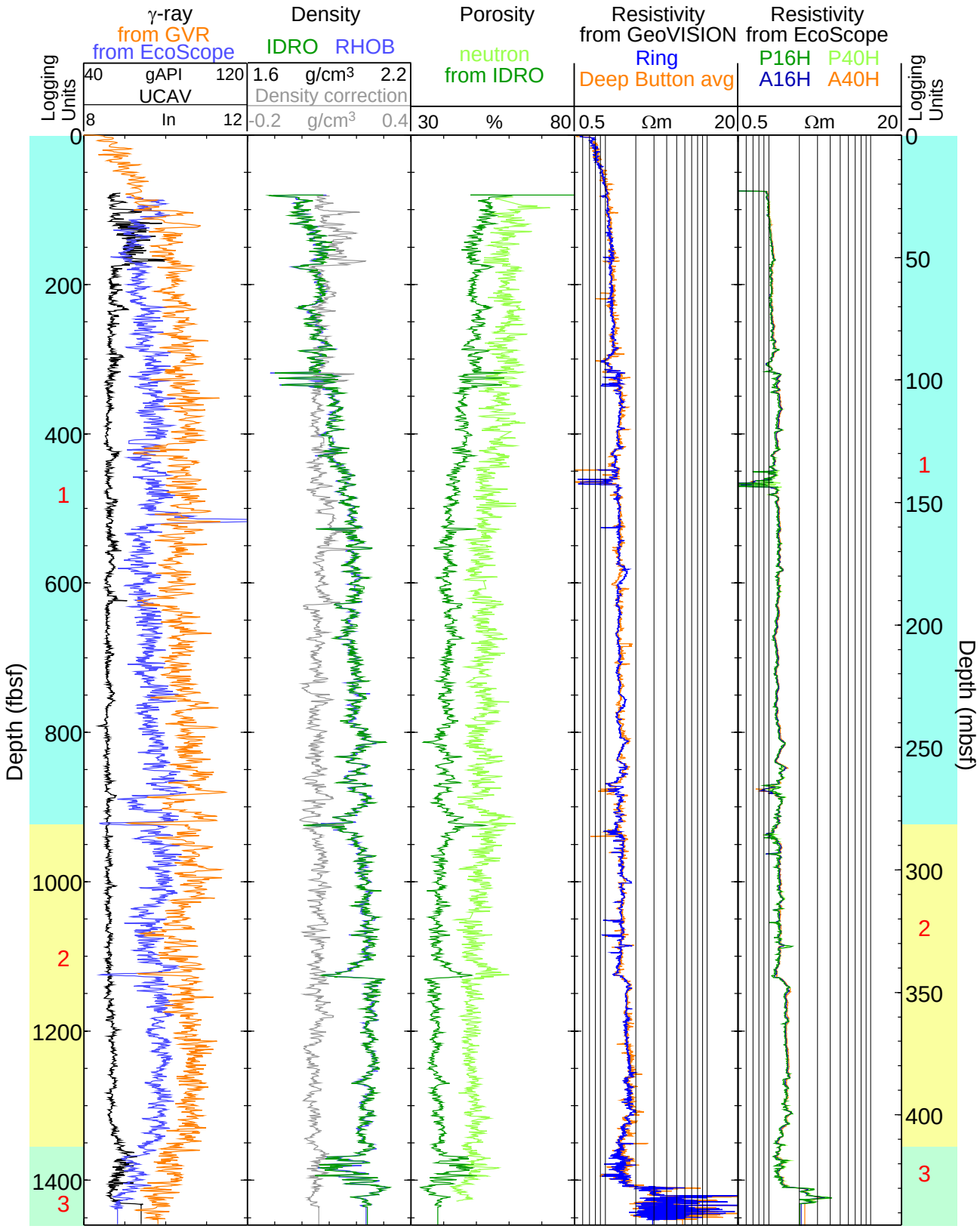

Figure F8: *Summary of LWD log data from Hole GC 955-Q. gAPI = American Petroleum Institute gamma ray units, RHOB = Bulk density (EcoScope), IDRO = Image-derived density (EcoScope); neutron = "Best neutron porosity" (EcoScope); Ring = Ring resistivity (geoVISION); PXXH = Phase-shift resistivity at 2 MHZ and a transmitter-receiver spacing of XX inches (EcoScope); AXXH = Attenuation resistivity measured at 2 MHz and a transmitter-receiver spacing of XX inches (EcoScope).*

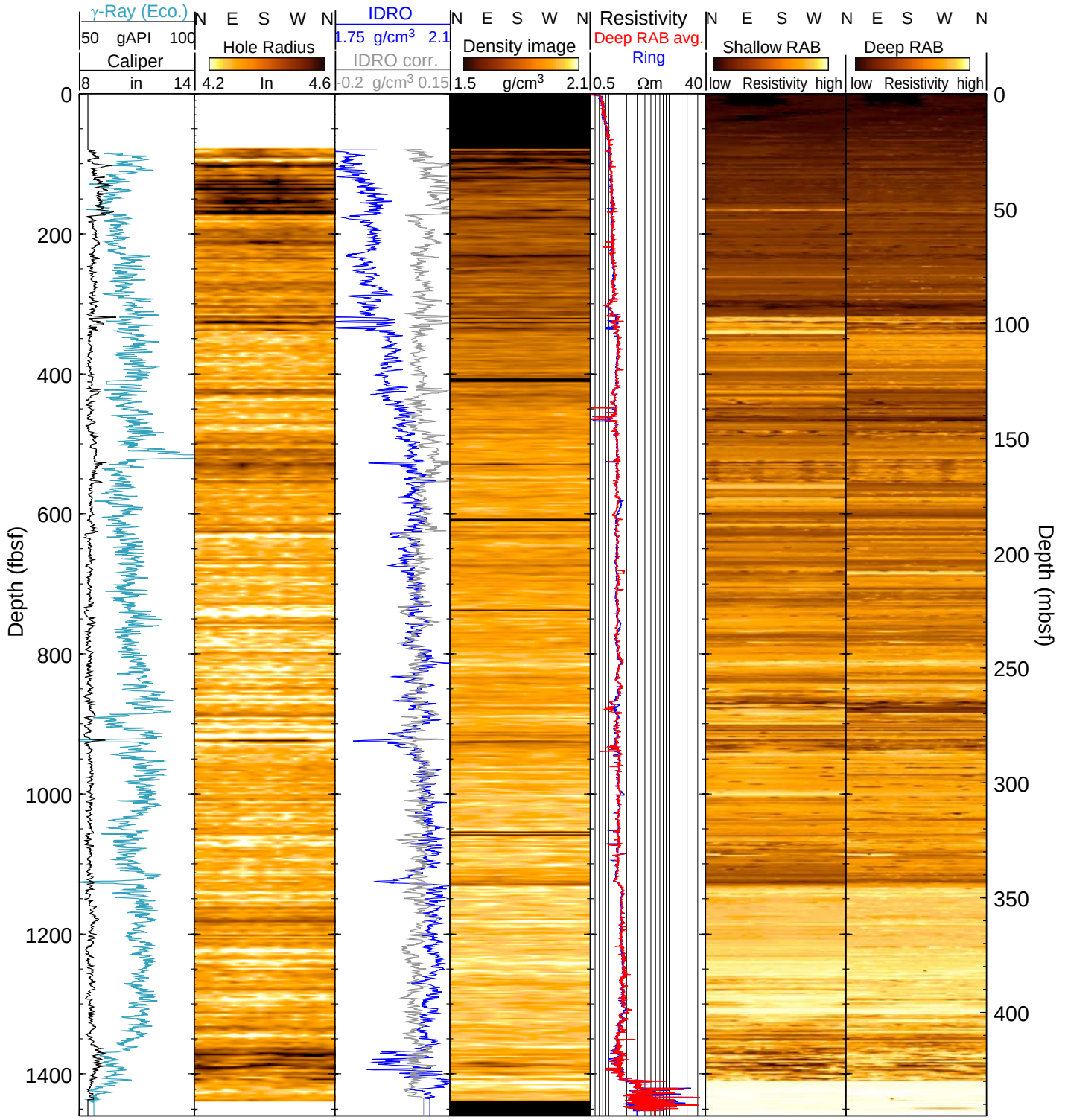

Figure F9: *LWD image data from Hole GC 955-Q. gAPI = American Petroleum Institute gamma ray units; RAB = Electrical image obtained by the geoVISION tool; IDRO = Image-derived density (EcoScope). The cardinal directions indicate orientation of the images.*

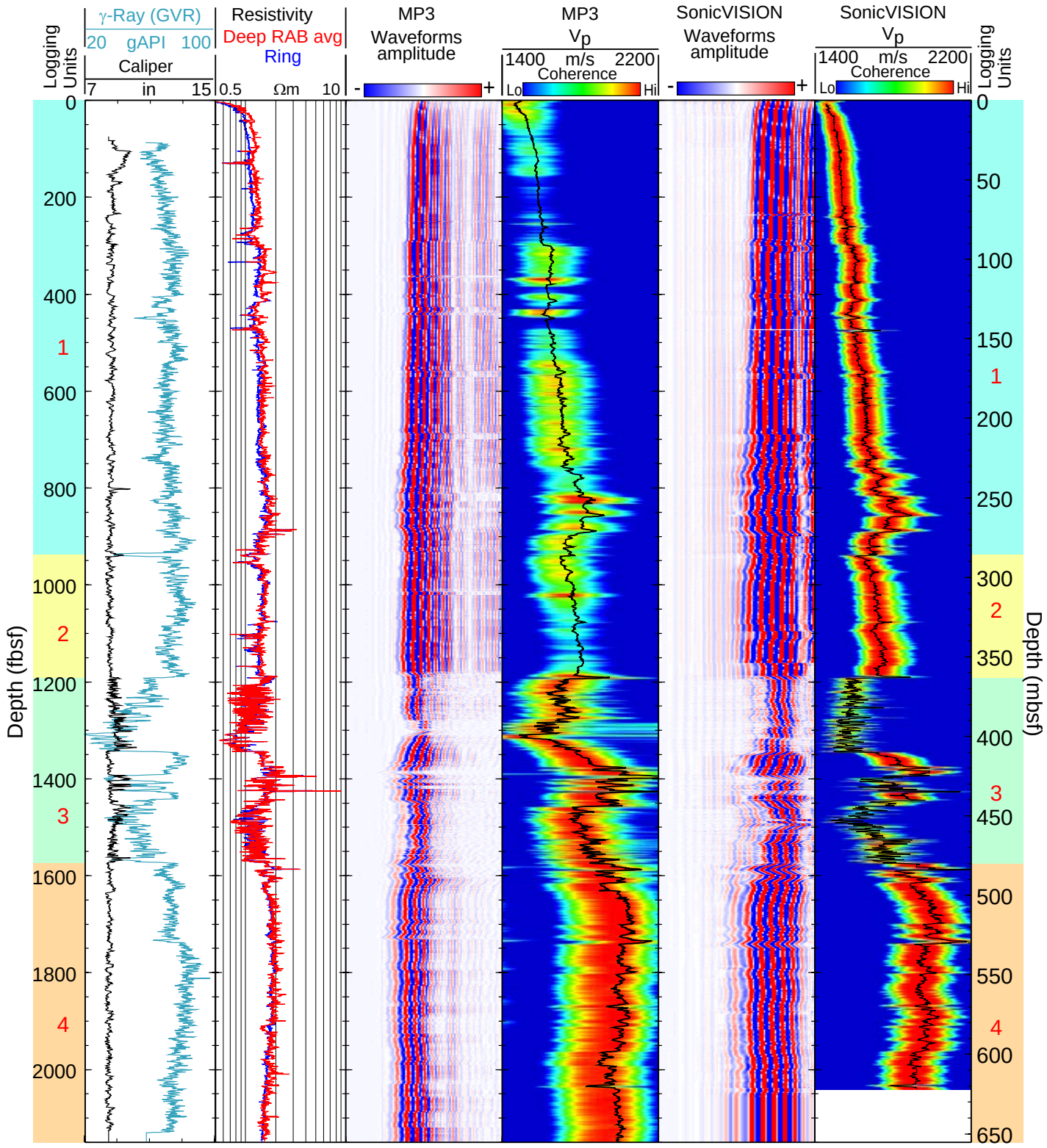

Figure F10: *Sonic waveform data and P-wave velocities recorded by the MP3 and sonicVISION sonic tools in Hole GC 955-I. Coherence projections resulting from the slowness-time coherence processing give an indication of the quality and reliability of the data. V_p = P-wave velocity. Logging Units as described in this report are shown.*

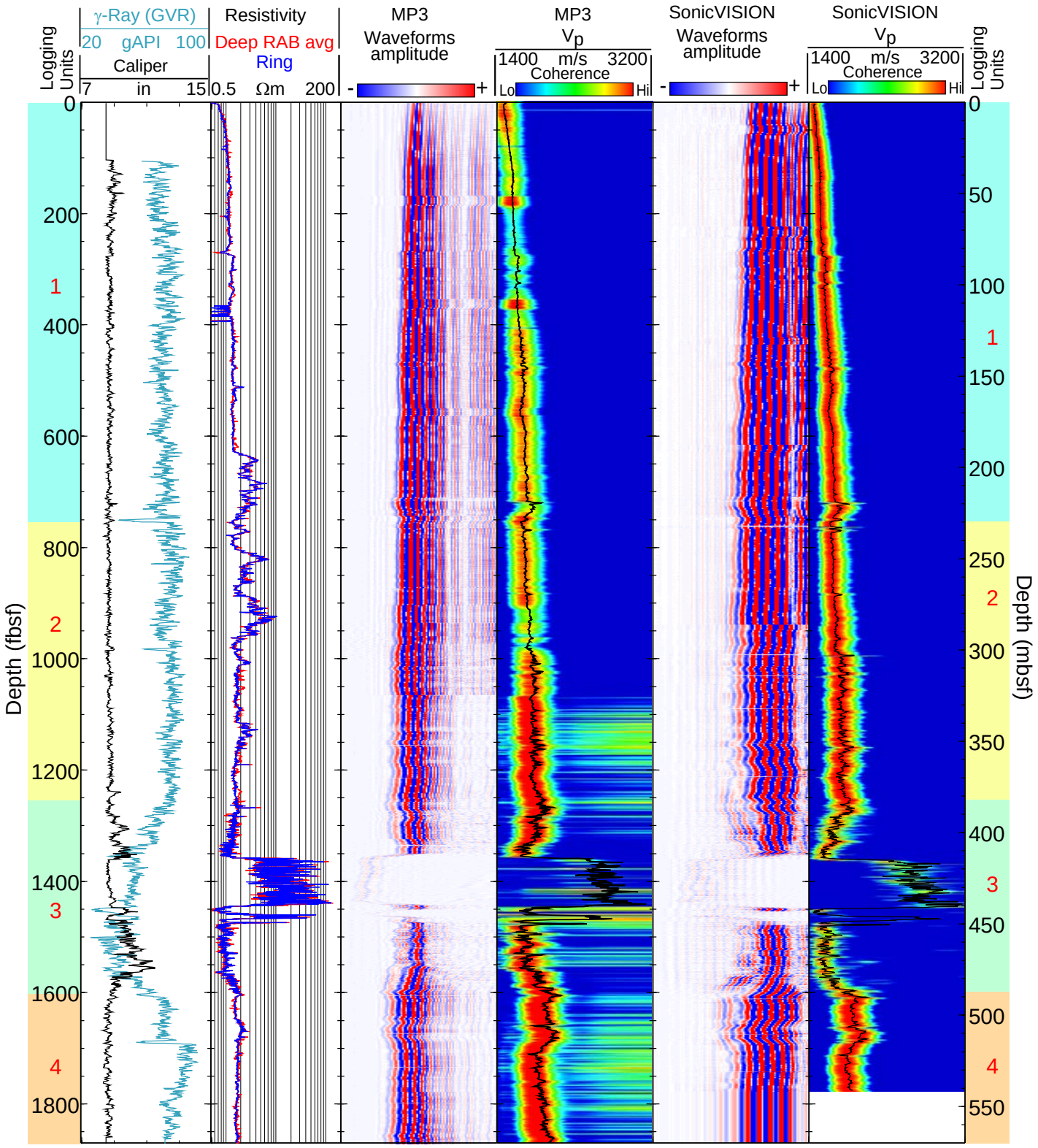

Figure F11: *Sonic waveform data and P-wave velocities recorded by the MP3 and sonicVISION sonic tools in Hole GC 955-H. Coherence projections resulting from the slowness-time coherence processing give an indication of the quality and reliability of the data. V_p = P-wave velocity. Logging Units as described in this report are shown.*

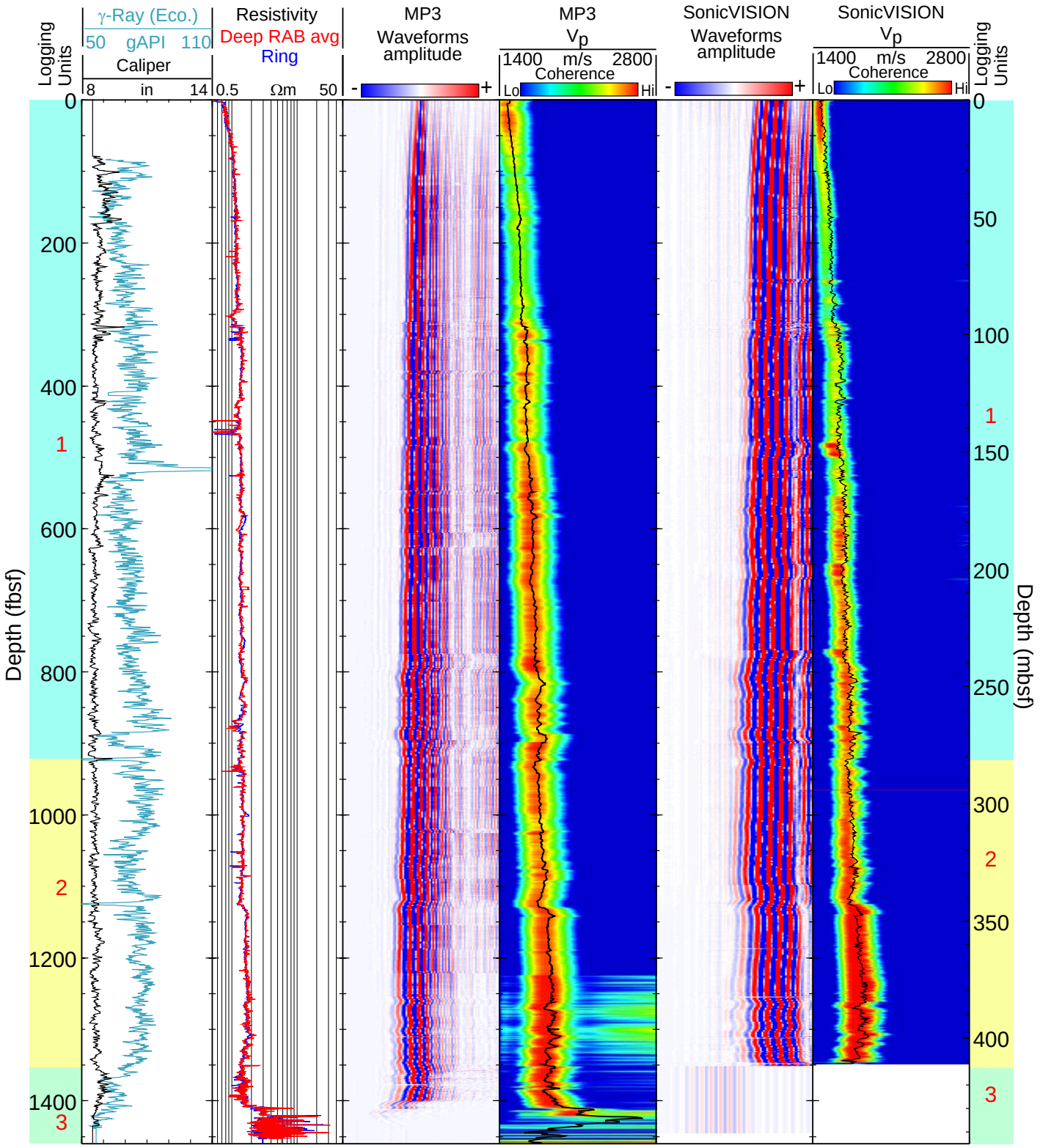

Figure F12: *Sonic waveform data and P-wave velocities recorded by the MP3 and sonicVISION sonic tools in Hole GC 955-Q. Coherence projections resulting from the slowness-time coherence processing give an indication of the quality and reliability of the data. V_p = P-wave velocity. Logging Units as described in this report are shown.*

Hole GC 955-H suggest that this well might be intersecting gas hydrate-filled fractures whithin Logging Units 1 and 2 (see ***LWD Borehole Images*** and ***Gas Hydrate*** below).

Logging Unit 3 is a sand-rich interval, characterized by lower gamma ray values, but also by enlarged hole conditions, particularly in Holes GC 955-I and GC 955-H as shown by the irregular caliper logs in Figures F2 and F5. The apparent low density and high porosity values are partially due to the enlarged hole. These sands were the main targets for the drilling program in this location, and proved particularly promising in the case of Hole GC 955-H, where high resistivity values between ~1350 and ~1450 fbsf are indicative of a high saturation hydrate-bearing sand section. The short high-resistivity interval logged at the bottom of the Hole GC 955-Q is also indicative of a hydrate-bearing sand reservoir. In Hole GC 955-I, gas hydrate could be present in a couple of thin sand layers within a more shaly section in the middle of Unit 3 (see ***Gas Hydrate*** below).

The top of Logging Unit 4 was reached only in Holes GC 955-I (at ~1575 fbrf) and GC 955-H (~1600 fbsf), where the hole diameter returns to normal and the gamma ray, density and velocity logs all return to values characteristic of the shallower clay formations. Except for a stepwise increase in gamma ray at ~1750 fbsf in GC 955-I and at ~1700 fbsf in GC 955-H indicating a transition to even more clay-rich sediments, most measurements remain uniform within Logging Unit 4 without any indication of either gas hydrate or free gas.

LWD Borehole Images

The geoVISION and EcoScope tools generate high-resolution images of borehole log data. The EcoScope tool produces images of density and hole radius (computed on the basis of the density correction, which is a function of borehole standoff), as well as gamma ray and photoelectric factor. The geoVISION produces a gamma ray image and shallow, medium and deep depth of investigation resistivity images.

Figures F3, F6, and F9 show some of the LWD images collected by the EcoScope and geoVISION tools in the Green Canyon 955 area. The unwrapped images are about 70 cm wide (for an 8.75 inch diameter borehole) and the vertical scale in these figures is highly compressed relative to the horizontal. Gas hydrate-bearing sediments exhibit high resistivity within intervals of uniform or low bulk density. By comparison, layers with high resistivities and high densities are likely to be low porosity, compacted, or carbonate-rich sediments.

The presence of gas hydrate is believed to stabilize the borehole (Tréhu *et al*., 2003). In Hole GC 955-H, one of the most prominent features is the high-resistivity interval between ~1350 and 1450 fbsf, within the sand-rich interval otherwise characterized by enlarged borehole (as indicated by dark areas in the hole radius image above and below this interval). In the high-resistivity interval, the hole quality does not seem to be affected by the high sand content of the sediments, suggesting that gas hydrate is increasing borehole stability.

Gas Hydrate

Each hole drilled in Green Canyon Block 955 has unique apparent gas hydrate occurrences. In Hole GC 955-I, only a few feet of the target sand display moderate resistivity excursions near 1400 fbsf (Figure F13). Hole GC 955-H crosses one large high resistivity sand interval from 1358 to 1445 fbsf (Figure F14) followed by a thinner high resistivity sand interval from 1460 to 1468 fbsf. In addition, Hole GC 955-H includes a large interval of apparent gas-hydrate-filled fractures in clay sediments between 630 and 960 fbsf (Figure F15), and one smaller interval between 1115 and 1142 fbsf. On the resistivity images, gas-hydrate-filled fractures appear as resistive sinusoids. Intervals containing high angle gas hydrate-filled fractures can be identified from the propagation resistivity measurements where the P40H and/or the A40H curves significantly exceed the P16H and A16H curves because of the electrical anisotropy due to the resistive fracture planes (Figure F5). Horizontal fractures or beds do not cause electrical anisotropy because logging tools are designed to detect horizontal features. Near the peaks and troughs of the resistive sinusoids, bright resistive halos can appear due to the current avoiding the path containing gas hydrate, often adjacent to dark conductive partial sinusoids where the current path is concentrated. In Hole GC 955-Q, high resistivities and velocities were measured in a sand interval from ~1410 fbsf to where the hole was terminated (Figure F16). The gas hydrate occurrence at GC 955-Q appears to be in a laminated sand section.

The techniques used to determine gas hydrate saturation from the measured resistivity are described in Mrozewski *et al*. (2009).

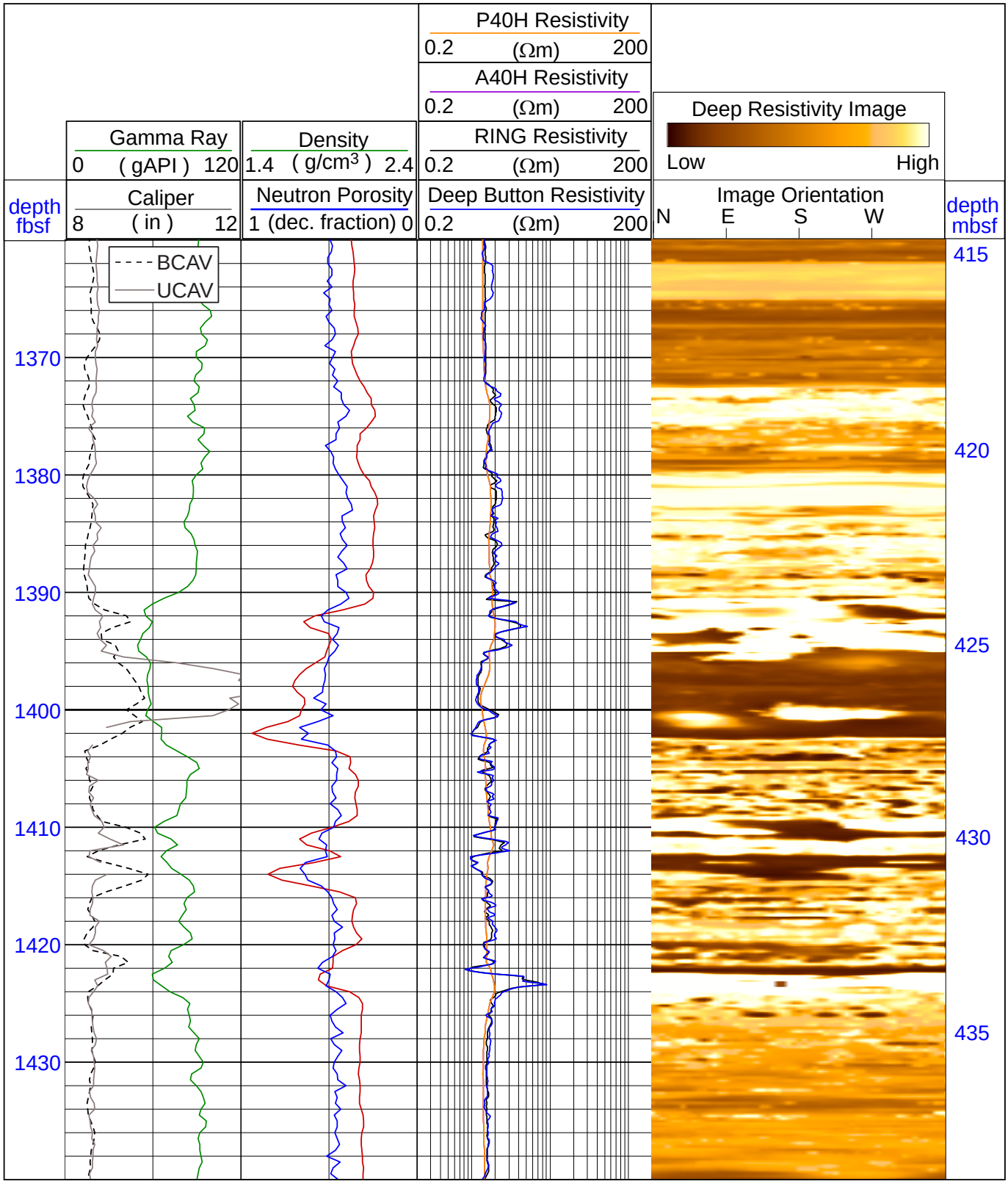

Figure F13: *Logs and LWD resistivity image from 1360 to 1440 fbsf in Hole GC 955-I showing the few feet of higher resistivity likely indicative of gas hydrate. Ring = Ring resistivity (geoVISION); P40H = Phase-shift resistivity at 2 MHZ and a transmitter-receiver spacing of 40 inches (EcoScope); A40H = Attenuation resistivity measured at 2 MHz and a transmitter-receiver spacing of 40 inches (EcoScope).*

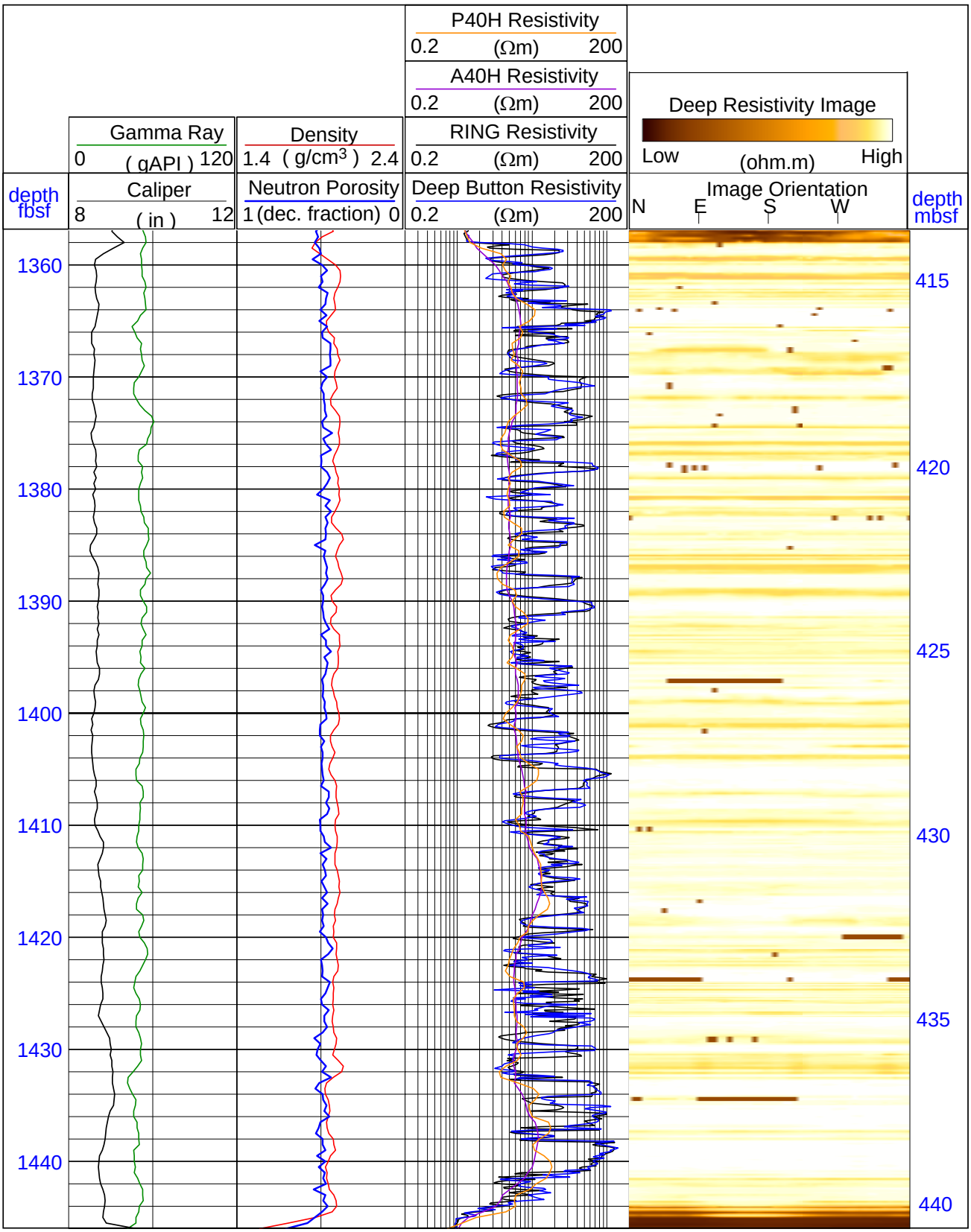

Figure F14: *Logs and LWD resistivity image from from 1358 to 1445 fbsf in Hole GC 955-H showing the target sand unit in this hole. Ring = Ring resistivity (geoVISION); P40H = Phase-shift resistivity at 2 MHZ and a transmitter-receiver spacing of 40 inches (EcoScope); A40H = Attenuation resistivity measured at 2 MHz and a transmitter-receiver spacing of 40 inches (EcoScope). The dark pixels in the high resistivity intervals are caused by a problem with the Schlumberger software.*

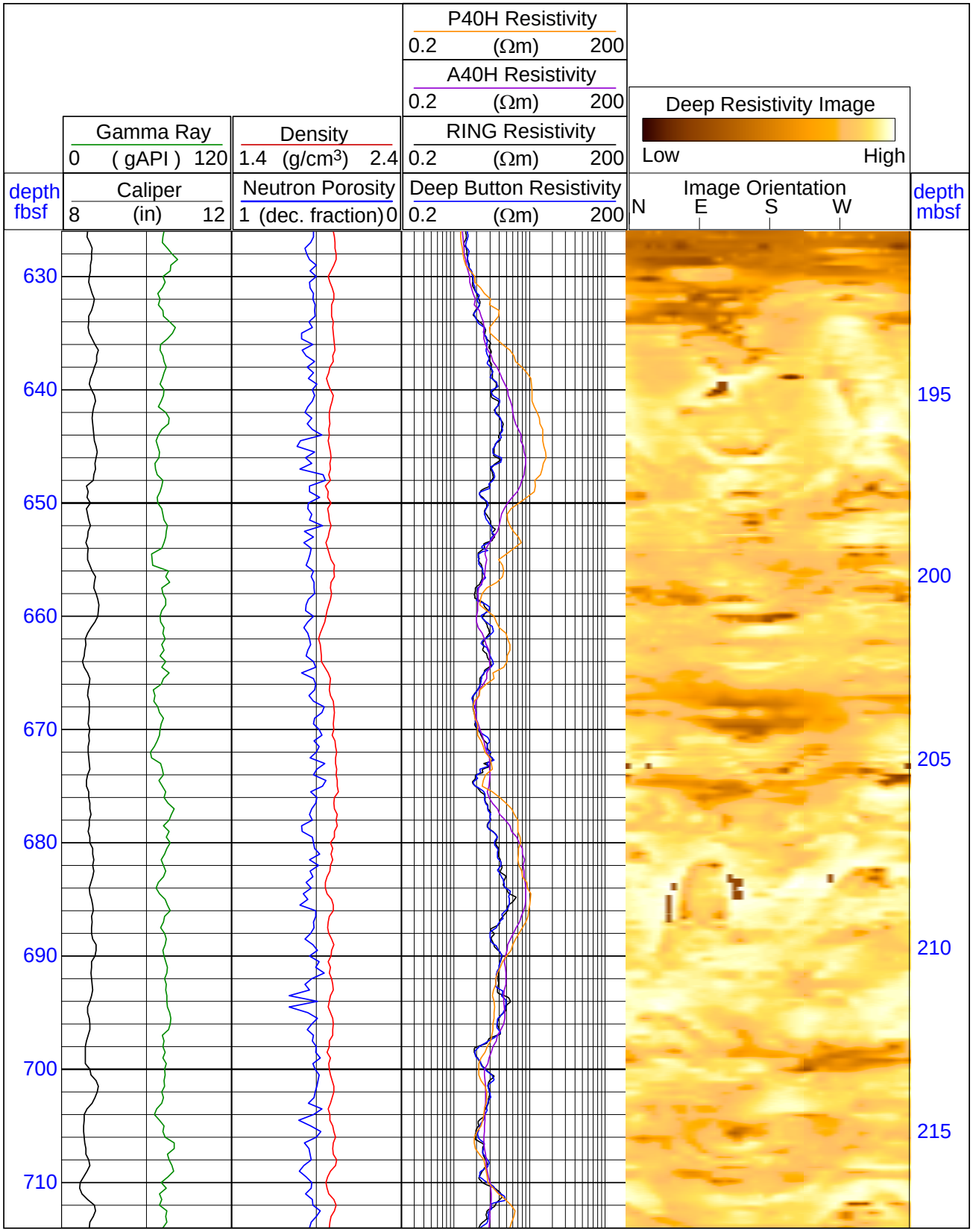

Figure F15: *Logs and LWD resistivity image from 626 to 714 fbsf in Hole GC 955-H showing steep high resistivity features that are likely high angle fractures filled with gas hydrate. Ring = Ring resistivity (geoVISION); P40H = Phase-shift resistivity at 2 MHZ and a transmitter-receiver spacing of 40 inches (EcoScope); A40H = Attenuation resistivity measured at 2 MHz and a transmitter-receiver spacing of 40 inches (EcoScope).*

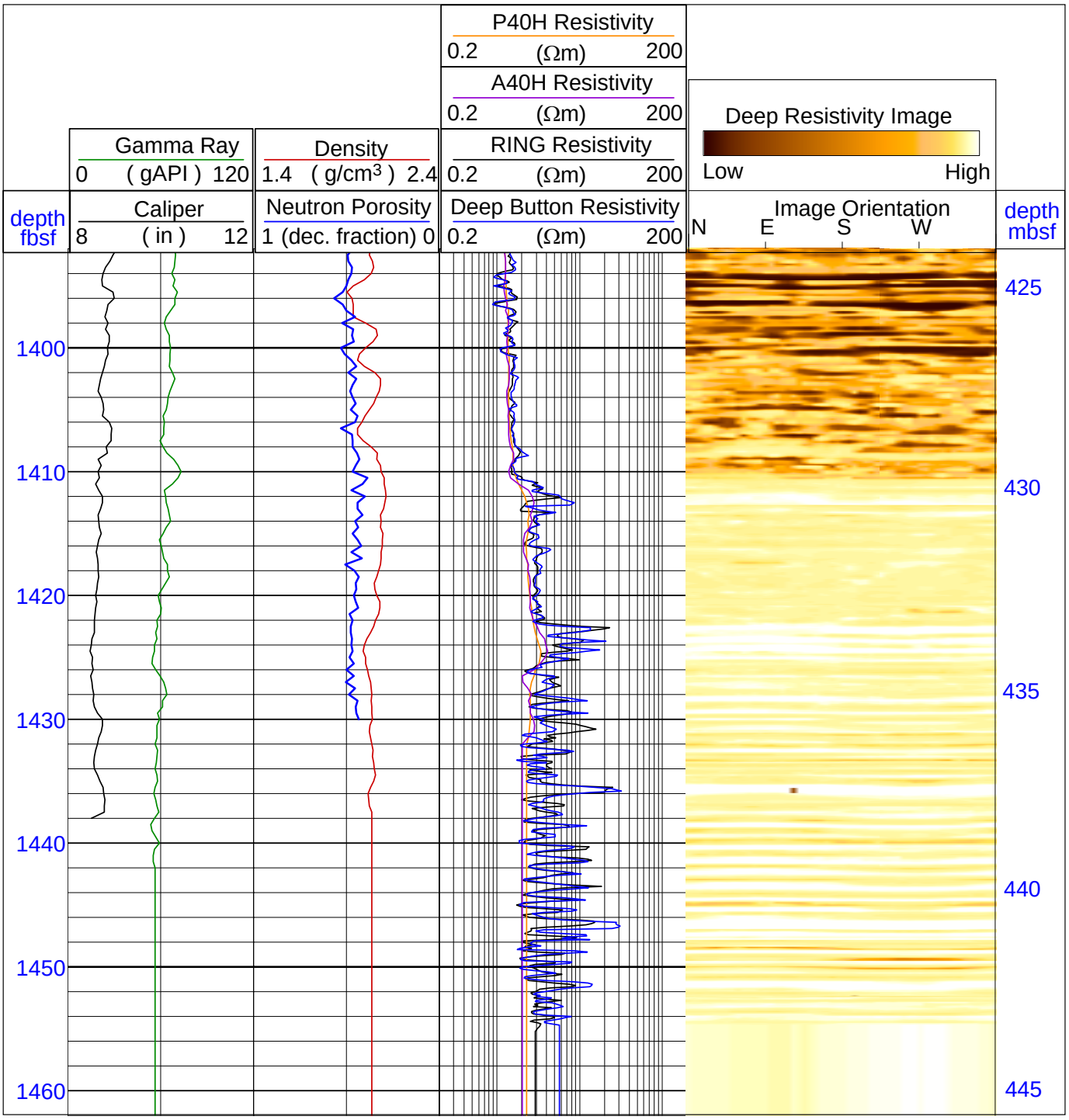

Figure F16: *Logs and LWD resistivity image from 1390 to 1460 fbsf in Hole GC 955-Q showing the few feet of higher resistivity at the bottom of the hole likely indicative of gas hydrate. Ring = Ring resistivity (geoVISION); P40H = Phase-shift resistivity at 2 MHZ and a transmitter-receiver spacing of 40 inches (EcoScope); A40H = Attenuation resistivity measured at 2 MHz and a transmitter-receiver spacing of 40 inches (EcoScope).*

In Hole GC 955-Q, the interval with the cleanest gamma ray (~65 API) and good hole conditions is between 887 and 906 fbsf. In this interval, the value of the cementation exponent m producing the best fit for $R_t = R_0 = (R_w/\backslash^m)$ is m = 1.8. The gamma ray log recorded only slightly lower API values, near 57 API, in the sand at the bottom of Hole GC 955-Q (Figures F17 and F18). The target sands in Hole GC 955-Q are thinly bedded, with the Archie analysis indicating the occurrence of interbedded hydrate sand units with variable gas hydrate saturations ranging between 40 and 75% to as low as ~20% in adjacent beds. The *m* value of 1.8 determined in Hole GC 955-Q was also applied to Holes GC 955-I and GC 955-H.

In Hole GC 955-I, a value of m = 1.8 was applied and a density approximation was used in the intervals with an enlarged hole (Figures F19 and F20). The density approximation was calculated by applying a linear fit to the density measurements of the sediments above and below the enlarged intervals. Only a small section of Hole GC 955-I contains gas hydrate, near 1400 fbsf, and Archie's equation suggests that most of this accumulation has a gas hydrate saturation < 50%.

In Hole GC 955-H, the high resistivity section of the target sands displays gamma ray readings of about 50 API. Given the extensive washout of the non-hydrate-bearing sands, no significant water-saturated sand intervals with low API exist with sufficiently-reliable log data for estimating m values in Hole GC 955-H. Thus, the value of m = 1.8 derived from GC 955-Q was applied for the target sand in GC 955-H. This is also the value providing the best fit for the water-saturated clays between 400 and 600 fbsf, which suggests that applying this value for m to the target sands is possibly in error. However, within the high resistivity range measured in Hole GC 955-H, the value of m has only a limited influence on the calculated gas hydrate saturation. Density measurements were not valid in the sand intervals with significant hole enlargements. The density values used for gas hydrate estimation in these intervals was derived from a linear fit of the density measured above and below the enlarged intervals (Figures F21 and F22). Within the target sands between 1358 and 1445 fbsf and between 1460 and 1468 fbsf, Archie's analysis suggests laminations with gas hydrate saturations > 70% alternating with laminations with gas hydrate saturations from 50 to 60%. In the intervals between 630 and 960 fbsf and between 1115 and 1142 fbsf, where it is inferred that gas hydrate is filling fractures, Archie's analysis suggests gas hydrate saturations ranging from 10% to 60%. However, current research suggests that Archie's equation in high-angle-gas-hydrate-filled fractures significantly overestimate gas hydrate saturation (Lee and Collett, 2009).

Conclusions

Drilling in three locations with distinct characteristics in Green Canyon Block 955 revealed various aspects of gas hydrate accumulation in this channel/levee system. The most important discoveries at Site GC 955 include:

- In Hole GC 955-I, gas hydrate only occurs in a few meters-thick sands around 1400 fbsf.
- In Hole GC 955-H, gas hydrate-filled more than 50% of the pore space in almost 100 ft of sands, and appears to cement the sands and promote hole stability.
- In addition, high-angle gas-hydrate-filled fractures occur in abundance over a ~300 ft interval in Hole GC 995-H.
- Only the top of the gas-hydrate-bearing sand was penetrated in Hole GC 955-Q, suggesting high concentrations of gas hydrate underneath.

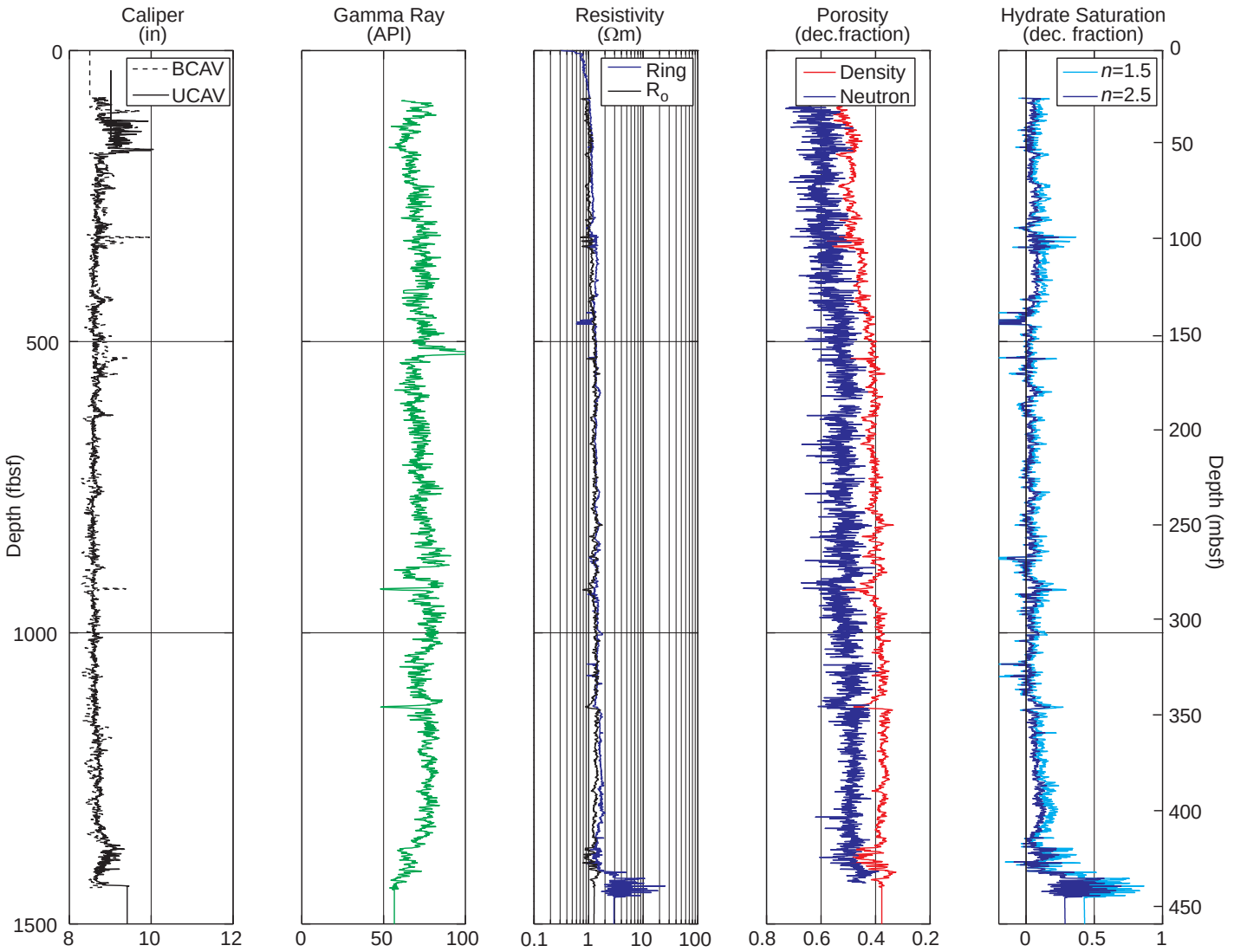

Figure F17: *Results of Archie's equation applied to the LWD porosity and resistivity logs in Hole GC 955-Q. BCAV = best density caliper; UCAV = ultrasonic density caliper; Ring = Ring resistivity (geoVISION); R_0 = Computed formation resistivity for 100% water saturation.*

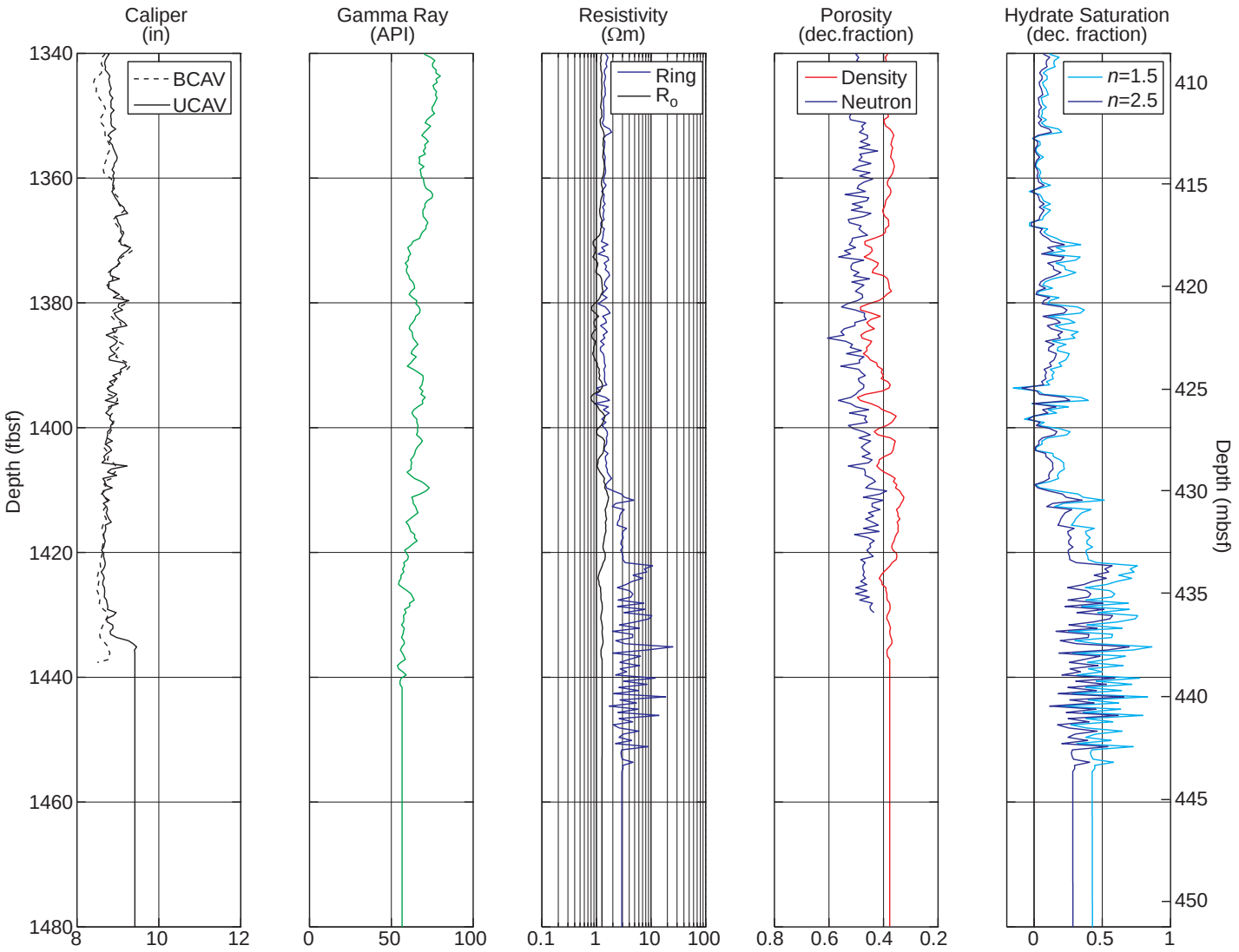

Figure F18: *Results of Archie's equation applied to the LWD porosity and resistivity logs in Hole GC 955-Q showing the top of the gas hydrate-bearing interval at the bottom of the hole. BCAV = best density caliper; UCAV = ultrasonic density caliper; Ring = Ring resistivity (geoVISION); R_0 = Computed formation resistivity for 100% water saturation.*

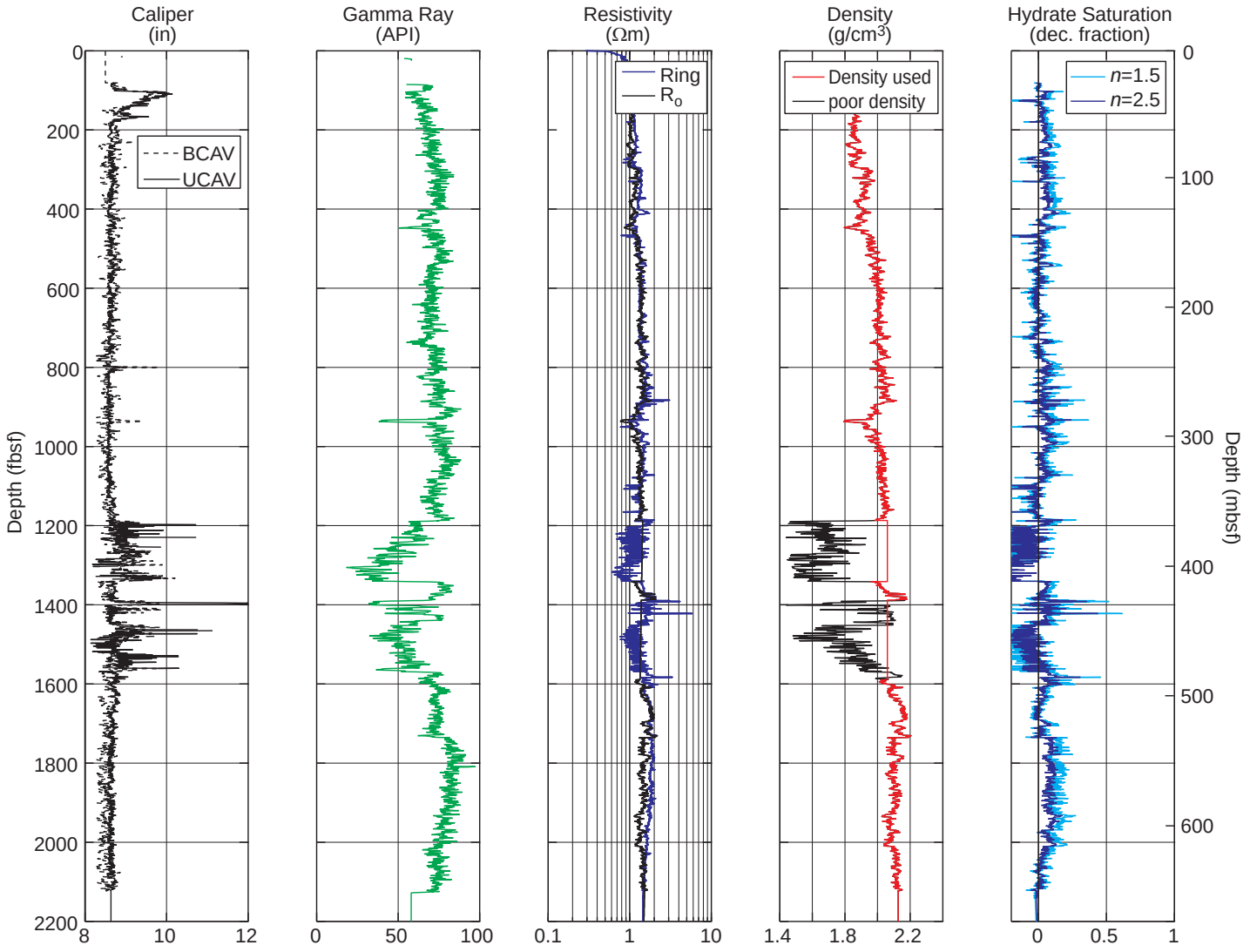

Figure F19: *Results of Archie's equation applied to the LWD porosity and resistivity logs in Hole GC 955-I. An average background density was used in sections with an enlarged borehole. BCAV = best density caliper; UCAV = ultrasonic density caliper; Ring = Ring resistivity (geoVISION); R_0 = Computed formation resistivity for 100% water saturation.*

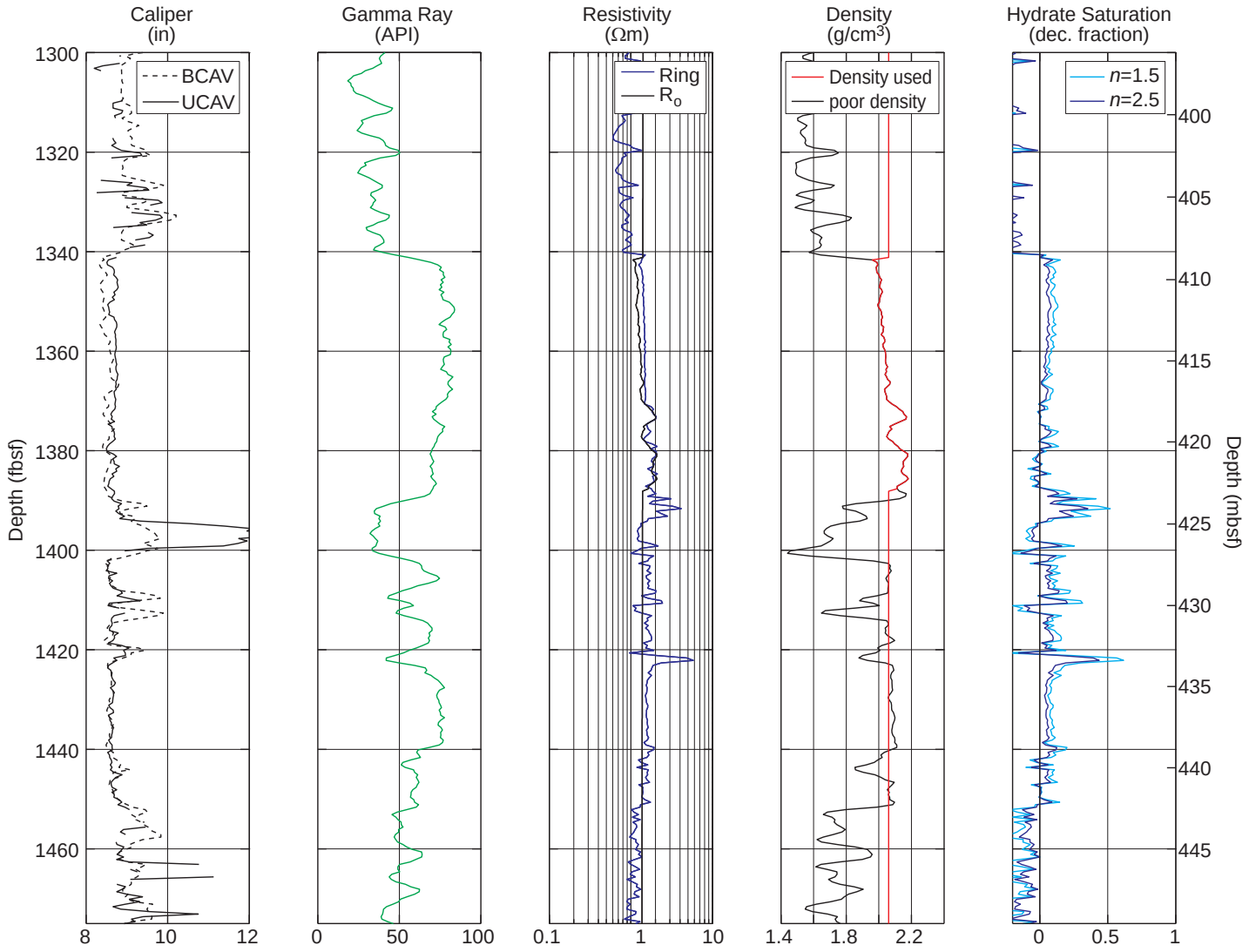

Figure F20: *Results of Archie's equation applied to the LWD porosity and resistivity logs displaying the few feet of hydrate-bearing formation in Hole GC 955-I. An average background density was used in sections with an enlarged borehole. BCAV = best density caliper; UCAV = ultrasonic density caliper; Ring = Ring resistivity (geoVISION); R_0 = Computed formation resistivity for 100% water saturation.*

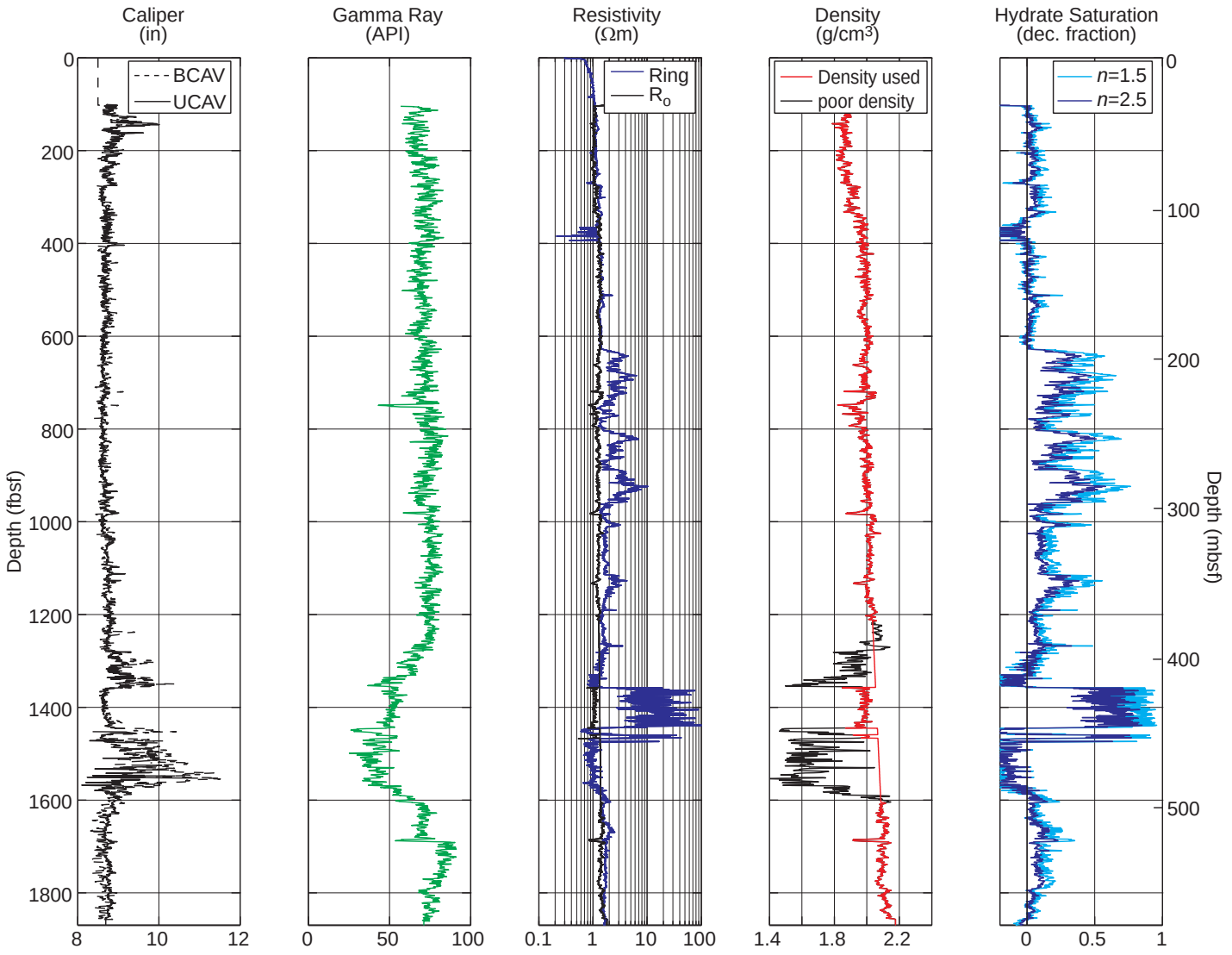

Figure F21: *Results of Archie's equation applied to the LWD porosity and resistivity logs in Hole GC 955-H. BCAV = best density caliper; UCAV = ultrasonic density caliper; Ring = Ring resistivity (geoVISION); R_0 = Computed formation resistivity for 100% water saturation.*

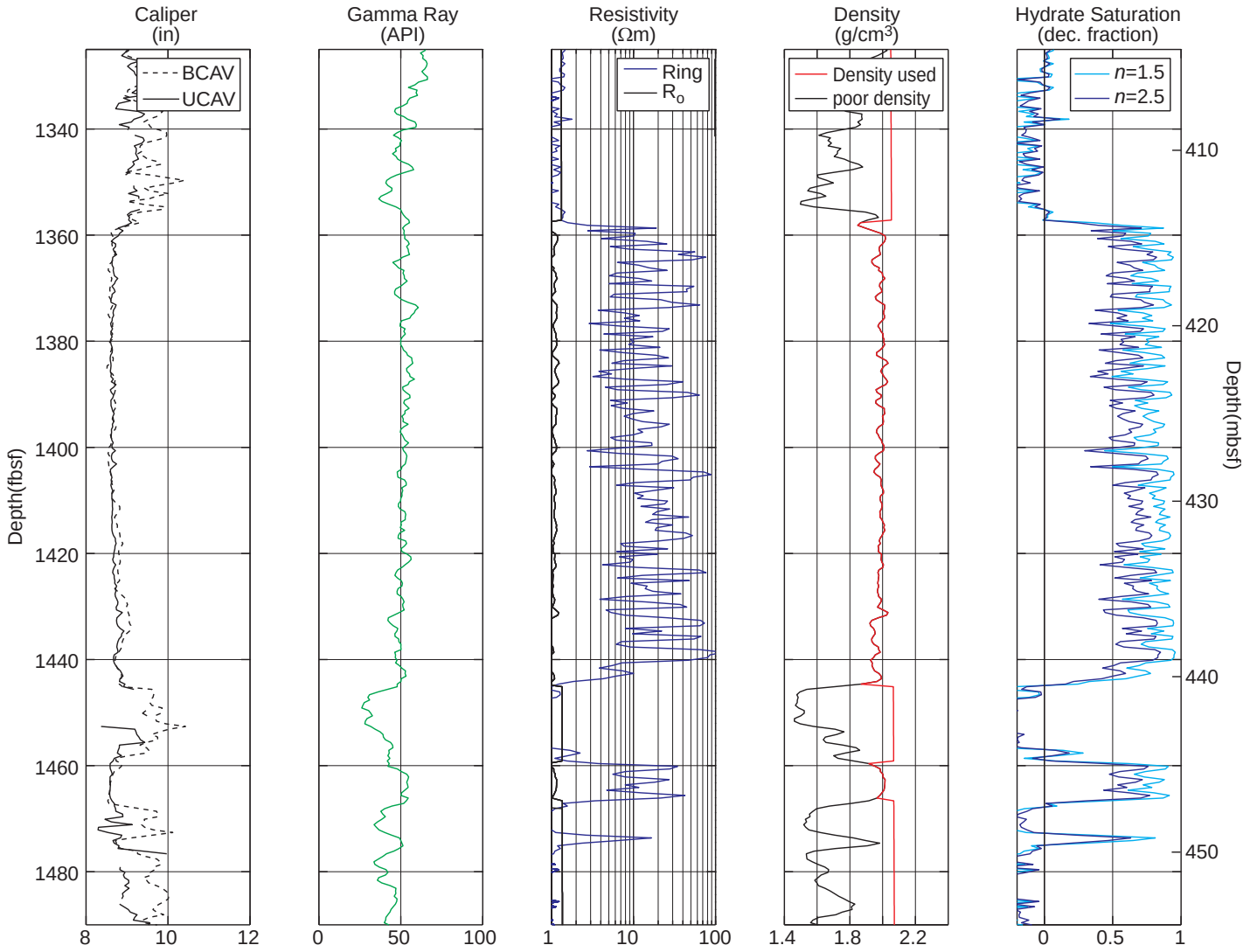

Figure F22: *Results of Archie's equation applied to the LWD porosity and resistivity logs in Hole GC 955-H for the target sand layers between 1358 and 1445 fbsf, and between 1460 and 1468 fbsf. BCAV = best density caliper; UCAV = ultrasonic density caliper; Ring = Ring resistivity (geoVISION); R_0 = Computed formation resistivity for 100% water saturation.*

References

Collett, T.S., Boswell, R., Mrozewski, S., Guerin, G., Cook, A., Frye, M., Shedd, W., and McConnell, D., 2009. Gulf of Mexico Gas Hydrate Joint Industry Project Leg II — Operational Summary: Proceedings of the Drilling and Scientific Results of the 2009 Gulf of Mexico Gas Hydrate Joint Industry Project Leg II. http://www.netl.doe.gov/technologies/oil-gas/publications/Hydrates/2009Reports/OpSum.pdf

Hutchinson, D., Boswell, R., Collett, T.S., Dai, J., Dugan, B., Frye, M., Jones, E., McConnell, D., Rose, K., Ruppel, C., Shedd, W., Shelander, D., Wood, W., 2009. Gulf of Mexico Gas Hydrate Joint Industry Project Leg II — Green Canyon 955 Site Selection: Proceedings of the Drilling and Scientific Results of the 2009 Gulf of Mexico Gas Hydrate Joint Industry Project Leg II. http://www.netl.doe.gov/technologies/oil-gas/publications/Hydrates/2009Reports/GC955SiteSelect.pdf

Lee, M. W. and T. S. Collett, 2009. Gas hydrate saturations estimated from fractured reservoir at Site NGHP-01-10, Krishna-Godavari Basin, India, J. Geophys. Res.114.10.1029/2008jb006237

McConnell, D., Boswell, R., Collett, T.S., Frye, M., Shedd, W., Guerin, G., Cook, A., Mrozewski, S., Dufrene, R., and Godfriaux, P., 2009. Gulf of Mexico Gas Hydrate Joint Industry Project Leg II — Green Canyon 955 Site Summary: Proceedings of the Drilling and Scientific Results of the 2009 Gulf of Mexico Gas Hydrate Joint Industry Project Leg II. http://www.netl.doe.gov/technologies/oil-gas/publications/Hydrates/2009Reports/GC955SiteSum.pdf

Mrozewski, S., Guerin, G., Cook, A., Collett, T.S., Boswell, R., 2009. Gulf of Mexico Gas Hydrate Joint Industry Project Leg II — LWD Methods: Proceedings of the Drilling and Scientific Results of the 2009 Gulf of Mexico Gas Hydrate Joint Industry Project Leg II. http://www.netl.doe.gov/technologies/oil-gas/publications/Hydrates/2009Reports/LWDMethods.pdf

Tréhu, A. M., *et al.*, 2003. Drilling Gas Hydrates on Hydrate Ridge, Cascadia Contiental Margin, College Station, TX (Ocean Drilling Program).